Non-volatile marine and non-refractory continental sources of particle-phase amine during the North Atlantic Aerosols and Marine Ecosystems Study (NAAMES)

Veronica Z. Berta[1], Lynn M. Russell[1], Derek J. Price[1,2], Chia-Li Chen[3], Alex K.Y. Lee[4], Patricia K. Quinn[5], Timothy S. Bates[5,6], Thomas G. Bell[7,8], Mike J. Behrenfeld[9]

[1]Scripps Institution of Oceanography, University of California, San Diego, La Jolla, CA 92093, USA
[2]Colorado Department of Public Health and Environment, Air Pollution Control Division, Denver, CO, 80246, USA
[3]California Air Resources Board, Riverside, CA 92507, USA
[4]Air Quality Processes Research Section, Environment and Climate Change Canada, Toronto, ON M3H 5T4, Canada
[5]NOAA Pacific Marine Environmental Laboratory, Seattle, WA 98115, USA
[6]Cooperative Institute for Climate, Ocean and Ecosystems Studies, University of Washington, Seattle, WA 98195, USA
[7]Plymouth Marine Laboratory, Plymouth, PL1 3DH, UK
[8]Department of Earth System Science, University of California, Irvine, CA, USA
[9]Department of Botany and Plant Pathology, Oregon State University, Corvallis, 97331 OR, USA.

Correspondence to: Lynn M. Russell (lmrussell@ucsd.edu)

Abstract. Amines were measured by aerosol mass spectrometry (AMS) and Fourier Transform Infrared (FTIR) spectroscopy during the North Atlantic Aerosols and Marine Ecosystems Study (NAAMES) cruises. Both AMS non-refractory (NR) amine ion fragments comprising the AMS $C_xH_yN_z$ family and FTIR non-volatile (NV) primary (C-NH2) amine groups typically had greater concentrations in continental air masses than marine air masses. Secondary continental sources of AMS NR amine fragments were identified by consistent correlations to AMS NR nitrate, AMS NR f_{44}, IC non-sea salt potassium, and radon for most air masses. FTIR NV amine group mass concentrations for particles with diameters <1 μm showed large contributions from a primary marine source that was identified by significant correlations with measurements of wind speed, chlorophyll *a*, seawater dimethylsulfide (DMS), AMS NR chloride, and ion chromatography (IC) sea salt as well as FTIR NV alcohol groups in both marine and continental air masses. FTIR NV amine group mass concentrations in <0.18 μm and <0.5 μm particle samples in marine air masses likely have a biogenic secondary source associated with strong correlations to FTIR NV acid groups, which are not present for <1 μm particle samples. The average seasonal contribution of AMS NR amine fragments and FTIR NV amine groups ranged from (27±57)% amine from primary marine sources and (73±152)% secondary continental amine during Early Spring to (53±76)% amine from primary marine sources and (47±68)% secondary continental amine during Winter. These results demonstrate that AMS NR and FTIR NV amine measurements are complementary and can be used together to investigate the variety and sources of amines in the marine environment.

1 Introduction

Amines are a class of nitrogen-containing organic compounds that have been identified as playing important roles in atmospheric aerosols by reacting with acids (HNO_3, H_2SO_4, MSA) to add organic mass and by acting as precursors that are

oxidized by atmospheric radicals (O_3, OH, NO_3) to nucleate new particles (Tang et al., 2013;Malloy et al., 2009;Bork et al.,

35 2014). New particle formation driven by amines can contribute to both the aerosol direct and indirect effects by increasing the number of particles as well as the number of cloud condensation nuclei (CCN) (Yao et al., 2018). Amines may also affect CCN activity by enhancing particle hygroscopicity through the formation of aminium salts or suppressing particle hygroscopicity through photochemical reactions with OH (Tang et al., 2014). The potential for climate impacts associated with amines depends strongly on the magnitude and type of amines in the atmosphere.

40

While continental sources of amine include animal husbandry, industrial emissions, and biomass burning (Ge et al., 2011), marine sources of aliphatic amines are likely underwater plant, algae, and kelp species, which are found in seawater and sediments (Lee, 1988;King, 1985;Steiner and Hartmann, 1968). These marine sources of amine have also been identified as both primary and secondary contributions to particles (Table 1). Marine amines are estimated to contribute 0.6 TgC/yr to

45 aerosol, and the formation of amine salts have been estimated to comprise 21% of submicron marine secondary organic aerosol (SOA) mass (Myriokefalitakis et al., 2010). Primary marine sources of amines have been identified, showing correlations to sea salt, wind speed, and alcohol groups (Frossard et al., 2014a;Lewis et al., 2022;Russell et al., 2011). Secondary marine sources of amine were identified for diethylamine, dimethylamine, and monomethylamine, which were correlated with primary productivity of phytoplankton (Facchini et al., 2008;Muller et al., 2009).

50

Fluxes of amine gases from the ocean to the atmosphere are controlled by biological activity because processes including osmoregulation, protein degradation, and subsequent microbial decomposition produce a methylated form of low-molecular-weight aliphatic amine that is concentrated in surface waters (Beale and Airs, 2016;King, 1985). This volatile form allows some amines to enter the atmosphere by air-sea exchange and then partition into the solid phase to form secondary marine

55 aerosols (SMA) by a variety of reactions. These reactions may be accelerated by airborne oxidants and other pollutants (NO_x, O_3, SO_x) that are transported from continental sources or produced by ships locally.

Amines are also included in primary sea spray aerosols (SSA) as jet and film drops of seawater that are ejected into the atmosphere by bursting bubbles formed by breaking waves at the ocean surface. These aerosol types have been associated with

60 biologically-derived marine organic compounds, since they frequently contain a consistent ratio of primary ($C-NH_2$) amine groups to organic mass across multiple oceans including the Arctic, Atlantic, and Pacific (Frossard et al., 2014a). Similar primary amine group contributions have been identified across four seasons in the North Atlantic in seawater, sea surface microlayer, generated primary particles, and atmospheric aerosol particles (Lewis et al., 2021;Lewis et al., 2022).

65 Here we assess the sources and quantities of amine components sampled in atmospheric aerosol particles during the North Atlantic Aerosols and Marine Ecosystems Study (NAAMES). NAAMES provided unique sampling of the open ocean during distinct seasons that correspond to different periods of the phytoplankton annual biomass cycle. To obtain the most complete

picture of open-ocean amines for the region, this study compares online measurements of AMS non-refractory (NR) amine fragments by High-Resolution Time-of-Flight Aerosol Mass Spectrometer (HR-ToF-AMS) to non-volatile (NV) primary amine groups by Fourier Transform Infrared Radiation (FTIR) Spectroscopy of size-resolved filters. Chemical and meteorological tracers are used to associate the amine components with both primary and secondary processes and marine or continental sources. Together, the AMS NR amine fragments and FTIR NV amine groups provide a more complete picture of the varied aspects of amine-containing aerosol particles in the North Atlantic.

2 Methods and Materials

2.1 NAAMES Cruises

The North Atlantic Aerosols and Marine Ecosystems Study (NAAMES) was a multi-year campaign that explored the dynamics of ocean ecosystems, atmospheric aerosols, clouds, and climate. The measurements reported here were collected on the R/V *Atlantis* in the western subarctic Atlantic during four separate phases of the phytoplankton annual biomass cycle (Behrenfeld et al., 2019). The first cruise (NAAMES 1) took place during the winter transition in November-December (Winter) 2015. The second cruise (NAAMES 2) took place during the transition in the bloom climax in May-June (Late Spring) 2016. The third cruise (NAAMES 3) took place during the declining biomass in August-September (Autumn) 2017. The final cruise (NAAMES 4) took place during the early accumulation phase of the spring bloom in March-April (Early Spring) 2018. The first three NAAMES cruises departed from Woods Hole, Massachusetts, and the NAAMES 4 cruise sailed from San Juan, Puerto Rico. All four cruises returned to Woods Hole, Massachusetts.

2.2 Marine and Continental Air Mass Periods

Ambient measurements were categorized by air mass origins. Online measurements were considered to be associated with marine air masses if they met the criteria of Saliba et al. (2020), namely (1) particle number concentrations <1,500 cm^{-3}, (2) HYSPLIT 48 hour back trajectories originating from the North or tropical Atlantic that did not pass over land during that time, (3) black carbon (BC) concentrations <50 ng m^{-3}, (4) radon concentrations <500 mBq m^{-3}, and (5) relative wind direction within ±90° of the bow of the ship (to avoid ship stack contamination). For the multi-hour filters collected, the classification scheme of Lewis et al. (2021) was used: marine filters were those for which 90% or more of the sampling time met these conditions; air masses were considered to have continental sources when the HYSPLIT 48 hour back trajectories originated from North America; mixed filters were those that did not meet either marine or continental criteria.

2.3 HR-ToF-AMS

A HR-ToF-AMS (Aerodyne Research Inc., Billerica, MA) was deployed to measure non-refractory (AMS NR) components of submicron (approximately 100-800 nm dry aerodynamic diameter) ambient particles (DeCarlo et al., 2006) downstream of a 1 μm cyclone (Russell et al., 2018). The HR-ToF-AMS vaporizer was operated around 600ºC. The instrument alternated

periodically between different ion flight modes including a high-resolution W-mode (1-min), a high-sensitivity V-mode (2-min), and an additional single-particle event trigger (ET) mode (2-min). Particle measurements with the W-mode of the AMS instrument were collected for all particles (not separated by size) and were analyzed by the data analysis software packages SQUIRREL (SeQUential Igor data RetRiEvaL) version 1.24 and PIKA (Peak Integration by Key Analysis) version 1.63 on IGOR PRO 8 (Wavemetrics, Inc.). This mode was used instead of the V-mode to obtain better peak separation, which was necessary to identify contributions of amine-containing fragments from other fragments at similar masses. SQUIRREL was used to pre-process data by checking m/z calibration and baselines for each run. PIKA was then utilized for high-resolution analysis of individual ion fragments to be fitted for each mass-to-charge ratio (m/z). AMS NR amine fragments were calculated as the sum of $C_xH_yN_z$ ion fragments (Schurman et al., 2015;Thamban et al., 2021). Figure S14 displays representative peak fittings of selected $CxHyN_z$ ion fragments.

The ET mode of the HR-ToF-AMS extracted a mass spectrum for individual particles that had ion signals within a certain range of m/z values that exceeded a threshold established using particle-free air. Single particle analysis of ET mode measurements was previously completed for Winter and Late Spring (Sanchez et al., 2018). This analysis was also performed for Autumn and Early Spring, identifying 5-7 relatively similar clusters for each cruise using criteria listed in Tables S8-S9. The AMS ET methods and results for Autumn and Early Spring are available in the Supporting Information Sections S2-3. Amine fragment contributions were estimated using the unit-mass fragments associated with common amine ion fragments (Tables S6-S7). The sum of these fragments was directly compared to the sum of $C_xH_yN_z$ ion fragments in Figure S6. The ten AMS NR single particle amine fragments with the highest mass concentrations were CHN^+, CH_4N^+, $C_2H_3N^+$, $C_2H_4N^+$, $CHNO^+$, $C_2H_5N^+$, $C_2H_6N^+$, C_4HN^+, $C_2H_5N_2O^+$, $C_3H_7NO^+$ (Figure S7). The fraction of amine signal that was associated with the Autumn and Early Spring particle clusters was estimated to be 1.0-3.6% of the total ion signal and for 2.7-8.1% of the total organic signal (Table S10). These contributions remained largely consistent across particle clusters, showing no notable differences between the particle clusters. Correlations of each particle cluster and selected tracers are displayed in Tables S11-S14 and a summary of these results can be found in Section S3. Time series and mass spectra of each single particle cluster are shown in Figures S8-S12.

Positive Matrix Factorization (PMF) Evaluation Tool v3.06B of W-mode data was used for Autumn and Early Spring to compute factors of ion fragments with unique temporal correlations for high-resolution organic mass spectral data, as described in Supporting Information Section S1. The analysis included selected high-resolution sulfate mass spectral signals that included SO^+, SO_2^+, SO_3^+, HSO^+, $H_2SO_4^+$, HSO_3^+, H_2SO^+, HSO_2^+, and $H_2SO_2^+$ ion fragments. The criteria used to determine the factor solution is listed in Tables S1-S4. Most of the factors identified typically included small amounts of amine; when a factor with higher amine contribution was found, the variability of its mass concentration was largely noise, limiting further source appointment, given the magnitude of twice that of its mean (Table S5). The time series and mass spectra of these factors are shown in Figure S1-S5.

The HR-ToF-AMS utilizes a multi-slit chopper that obtains efficient Particle Time-of Flight (ePToF) measurements rather than a single-slit chopper that obtains PToF measurements. ePToF ensures high signal-to-noise ratios in the raw spectral bins necessary for marine environments with low aerosol concentrations. ePToF measurements can be analyzed as size distributions of individual unit-mass resolution ion fragments but processing of high-resolution mass spectra for separate size bins has not yet been implemented. Size distributions of cumulative and individual mass fragments for organic and sulfate fragments had low signal-to-noise given the clean marine conditions and low concentrations of AMS NR components. Unit mass resolution did not represent any of the selected amine fragments with sufficiently high signal-to-noise to determine an amine size distribution or size cuts (e.g. <0.5 μm), as the amine fragments comprised less than half of the unit mass resolution peaks in the m/z spectra (Table S7). Consequently size-resolved measurements of AMS NR amine fragments are not available.

2.4 FTIR Spectroscopy

During all four cruises, atmospheric particles were collected after size cuts on pre-scanned 37 mm Teflon filters (Pall Inc., 1 μm) for offline analysis by Fourier Transform Infrared (FTIR) spectroscopy (Tensor 27 spectrometer, Bruker, Billerica, MA) of the NV components that were retained on the filters (Russell et al., 2018). Berner impactors with size cuts of 0.18 μm and 0.5 μm were operated at 30 L min^{-1}, and a 1 μm sharp cut cyclone was operated at 16.7 L min^{-1}. Sampling times for each filter spanned 12 to 23 hours. A sector control was used for filter sampling (Lewis et al., 2021). Quantification of NV organic amine group concentration was accomplished by identifying a primary amine (C-NH_2) peak at an absorption frequency of 1630 cm^{-1} in the FTIR spectrum. Note that the term 'primary' refers to the NH_2 group type that is bonded to the carbon not to the aerosol source type. Specifically, the FTIR absorbance at 1630 cm^{-1} is not sensitive to secondary (C_2-NH) or tertiary (C_3-N) groups in amines, and absorbance peaks for secondary and tertiary amines were not identified in the spectra (Kamruzzaman et al., 2018). The FTIR spectra were quantified by baselining, peak-fitting, and integrating peak areas using calibration standards and an automated algorithm (Maria et al., 2002). Carboxylic acid, alkane, primary amine, and alcohol functional groups were estimated from fitting spectral peaks as described in detail by (Takahama et al., 2013;Lewis et al., 2021).

2.5 Ion Chromatography

Inorganic ions including SO_4^{2-}, NO_3^-, NH_4^+, Na^+, MSA, Mg^{2+} K^+, Cl^-, Ca^{2+}, and Br^- were collected on a two stage multi-jet impactor with a 1.1 μm size cut filter at 30% RH and subsequently measured using ion chromatography (IC) (Quinn et al., 1998). Sea salt concentrations were estimated as Na^+ (μg m^{-3}) ×1.47 + Cl^- (μg m^{-3}) (Saliba et al., 2020;Frossard et al., 2014a;Bates et al., 2012;Quinn et al., 2019). Non-sea salt (nss) potassium (K^+) concentrations were estimated as K^+ (μg m^{-3}) - Na^+ (μg m^{-3}) × (ratio of K to Na in seawater), where the latter ratio is constant across major water masses in the ocean (Pilson, 2013).

2.6 Other Measurements

Seawater and atmospheric dimethylsulfide (DMS) concentrations were measured continuously during NAAMES (Bell et al., 2021). Chlorophyll a was also measured inline using High Performance Liquid Chromatography (HPLC). A Single Particle
165 Soot Photometer (SP2, DMT, Boulder, CO) measured the mass concentrations of refractory black carbon (BC) in particles with diameters of 60 to 700 nm. Other meteorological properties measured during NAAMES and used in our analysis include sea surface temperature (SST), solar radiation, wind speed, relative humidity, ambient temperature, ozone, and radon and these data, in addition to chlorophyll a, were accessed from the SeaBASS archive (Werdell et al., 2003). A thermodenuder Scanning Mobility Particle Sizer (SMPS) measured submicron particle size distributions and a Cloud Condensation Nuclei Counter
170 (CCNC, DMT, Boulder, CO) measured ambient CCN concentrations at 0.1% supersaturation. Aerosol hygroscopicity was estimated from SMPS and CCNC measurements during Autumn and Early Spring (SI Section S5), but the available CCN measurements were too sparse to identify a relationship with composition (Table S21).

3 Results

Figure 1 shows AMS NR amine fragments and FTIR NV amine groups for all four NAAMES cruises. Concentrations of both
175 amine measurements varied substantially during each cruise, but median and mean amine concentrations (Tables 2 and 3, respectively) had similar differences between air masses for AMS NR amine fragments and FTIR amine groups. Concentrations of AMS NR amine fragments were higher during continental periods (with concentrations ranging from 18 to 54 ng m^{-3}) than during marine periods, when concentrations averaged below 33 ng m^{-3}, except for Early Spring (Table 2). Winter, Late Spring, and Autumn were statistically significant ($p < 0.05$, two-sample Student's t-test). Similar to AMS NR
180 amine fragments, FTIR NV amine group concentrations were higher overall during continental periods, highlighting that continental transport is a significant source of amines in the North Atlantic. The average FTIR NV amine group concentration ranged from 7 to 18 ng m^{-3} during marine periods and from 16 to 33 ng m^{-3} during continental periods (including filters with amine below the detection limit). However, the differences in average FTIR NV amine group concentrations between marine and continental air masses were only statistically significant during Winter.

185

Notwithstanding the above consideration on continental transport, concentrations of AMS NR amine fragments were lowest in Winter, when AMS NR organic mass (OM) was also lowest and IC MSA concentrations were below detection for both marine and continental air masses. These low concentrations of 14 to 18 ng m^{-3} in Winter may indicate that biologically-derived amine makes up a significant fraction of non-refractory amine during other seasons, since primary production has
190 previously been shown to influence amine concentrations in the North Atlantic (Muller et al., 2009). The highest concentration of AMS NR amine fragments for marine periods was 33 ± 6 ng m^{-3} in Early Spring and for continental periods 54 ± 49 ng m^{-3} in Autumn. For marine air masses, FTIR NV amine groups were highest in Late Spring, but, for continental air masses, FTIR

NV amine groups were highest in Winter. FTIR NV amine group concentrations were lowest for both marine and continental air masses in Early Spring, when only two filters, both with FTIR NV amine groups below detection, met the marine criteria.

195

Average concentrations of FTIR NV amine groups were lower than concentrations of AMS NR amine fragments, except for the continental period in Winter. Two campaigns had positive, but not statistically significant, correlations of FTIR NV amine groups with AMS NR amine fragments, with R = 0.45 in Winter and R = 0.87 in Autumn. The two Spring campaigns had negative correlations of FTIR NV amine groups and AMS NR amine fragments that were not statistically significant (Fig.2).

200 Consequently, combining the four cruises for both air mass types gives no correlation between FTIR NV amine groups and AMS NR amine fragments ($\rho = 0.02$, where a Spearman's rank correlation coefficient was used for the non-normal distribution of FTIR NV amine groups and AMS NR amine fragments). This result suggests that FTIR and AMS are measuring different amine compounds, likely associated with different source types. In particular, AMS measures non-refractory components and FTIR measures non-volatile components (but some amine compounds are on refractory sea spray particles and some amines

205 volatilize from filters). The inability of AMS to detect refractory components that are found mixed with sea spray particles is another reason that amine measured by FTIR and AMS are from different sources (Frossard et al., 2014b). The non-zero y-intercepts of AMS NR amine fragments to FTIR NV amine groups in Figures 2b-2e further support the interpretation that AMS and FTIR are measuring different amine compounds.

210 AMS NR amine fragments had moderate to strong correlations (0.73 < R < 0.98, Table 4) with AMS NR OM, suggesting that many of the organic sources included a consistent fraction of amines. The weak correlation for the marine period in Early Spring may reflect sources with different contributions of AMS NR amine fragments to AMS NR OM. FTIR NV amine groups had some weak correlations to AMS NR OM (-0.66 < R < 0.54, Table 5) but moderate to strong correlations to FTIR NV OM (0.69 < R < 0.96) in all seasons when filters were available (with the exception of Late Spring continental periods). Correlations

215 of FTIR NV amine groups to AMS NR amine fragments in continental and marine air masses were variable across individual seasons.

4 Discussion

4.1 Marine Amine Sources

FTIR NV amine functional groups have been reported in atmospheric aerosol, generated primary marine aerosols, seawater,

220 and the sea surface microlayer sampled during conditions when air masses were considered clean marine in the North Atlantic, with their presence in both seawater and aerosols supporting that those amines are largely from sources that are both primary and marine (Lewis et al., 2022;Frossard et al., 2014a). FTIR NV amine groups indicate an association with sea spray (Saliba et al., 2019) because of their positive (0.49 < R < 0.52, Figure 3h) correlations to wind speed during continental periods in Winter and Early Spring, which included the highest wind speeds during NAAMES. The correlations with FTIR NV amine

groups were not significant due to the limited number of samples (Table S16). AMS NR amine fragments did not correlate positively to wind speed (Figure 4c,d), consistent with the expectation that amines from primary marine sources would be mixed with refractory sea salt particles (Hawkins et al., 2010;Frossard et al., 2014b). The absence of a positive correlation with wind speed may be attributed to differences in local and upwind wind speeds, but the presence of negative correlations indicates a source of AMS NR amine fragments that is not associated with sea salt. The p-values corresponding to correlations of AMS NR amine fragments are displayed in Table S15. The limited number of points in each correlation of AMS NR amine fragments and FTIR NV amine groups are shown in Tables S19 and S20, respectively.

Additional markers for a primary marine source include IC sea salt and AMS NR chloride. While AMS NR amine fragments correlated moderately ($0.59 < R < 0.65$, Figure 4e,f) with IC sea salt for marine air masses in Winter and Autumn, FTIR NV amine groups showed low to moderate correlations ($R = 0.33\text{-}0.64$, Figure 3e,f) to IC sea salt during the marine period in Late Spring and Autumn and even a strong correlation ($R = 0.78$) during the continental period in Early Spring. The FTIR NV amine group measurements include some low concentrations and few samples, meaning that these correlations are uncertain and not significant. FTIR NV amine groups correlated moderately ($0.57 < R < 0.76$, Figure 3a,b) with AMS NR chloride during both continental periods (Winter and Early Spring) and two of the three marine periods (Winter and Autumn) for which measurements were available. Although these correlations of FTIR NV amine groups and AMS NR chloride are only significant ($p < 0.05$) for the continental Winter period, the consistency of their positive correlations contrast with the absence of correlation ($-0.15 < R < 0.13$, Table 4) between AMS NR chloride and AMS NR amine fragments during all four NAAMES cruises.

Chlorophyll a (chl a) is a common proxy for phytoplankton productivity that has previously been found to strongly correlate with organic mass in sea spray aerosols in coastal Atlantic regions (O'Dowd et al., 2004), but during NAAMES there was no clear dependence for <1 μm OC samples and a weak dependence for <1 μm OM cruise averages (Bates et al., 2020;Saliba et al., 2020). Consistent with these prior open ocean results for OM during NAAMES, no positive correlations were found for AMS NR amine fragments and chl a, or for FTIR NV amine groups in most of the cruises. The exception was a strong ($R = 0.85$, Figure 3g) correlation for FTIR NV amine groups during the marine period in Late Spring, which is the climax of the annual phytoplankton bloom. This finding is analogous to that of Russell et al. (2010) who attributed a weak, positive correlation of organic mass with chl a to particulate organic carbon (POC) in marine particles in bloom regions in the North Atlantic. The lack of correlations of organic mass and chl a is consistent with the less variable DOC pool as a carbon source for marine particles, as DOC typically does not correlate to chl a (Carlson et al., 1994). Therefore, these correlations with chl a support a primary marine source for FTIR NV amine groups.

The production of methylated amines and sulfurs varies with individual metabolic processes and across different ocean phytoplankton species (Keller, 1989;Liu et al., 2022a). Similar to methylated sulfurs, a significant portion of methylated

amines are derived from phytoplankton and subsequent biological degradation (Mausz and Chen, 2019). While chlorophyll *a* is produced by various phytoplankton species for photosynthesis, dimethylsulfide (DMS) is primarily produced by coccolithophores (Malin et al., 1993). Therefore, DMS may serve as an alternative tracer for ocean biological production in addition to chl *a*. FTIR NV amine groups correlated positively ($0.54 < R < 0.85$, Figure 3c,d) with seawater DMS during the marine period in Late Spring and the continental period in Winter. During these same periods, correlations of atmospheric DMS and FTIR NV amine groups were weakly positive ($0.26 < R < 0.46$) and lower than the correlations of FTIR NV amine groups to seawater DMS. The weaker correlation with atmospheric than seawater DMS may be explained by the photochemical reactions of atmospheric DMS leading to daytime concentration decreases that are lagged by the peaks in concentration of FTIR NV amine groups. No correlations of seawater DMS to AMS NR amine fragments were observed. This is a distinct difference from FTIR NV amine groups that suggests the seawater DMS is more correlated to seawater organic components (DOC or POC) rather than secondary organic components, and that those seawater organic components are emitted on refractory sea spray particles that are not measured by AMS. Weak to moderate correlations ($0.36 < R < 0.50$, Figure 4a,b) of atmospheric DMS and AMS NR amine fragments were observed during continental periods in Winter and Autumn and during the marine period in Early Spring, consistent with a secondary contribution to the AMS NR amine fragments that is distributed on AMS NR particles rather than sea salt. In summary, correlations of seawater DMS suggest a primary marine source for FTIR NV amine groups but not for AMS NR amine fragments.

Methanesulfonic acid (MSA), an oxidized derivative of DMS, can serve as a reliable indicator of secondary atmospheric processing, since its formation also lags atmospheric DMS concentrations (Sanchez et al., 2018). MSA may also react with alkylamines in acid-base reactions, similar to nitric acid (Chen et al., 2015;Chen et al., 2016;Chen and Finlayson-Pitts, 2017;Perraud et al., 2020). During marine periods, correlations between IC MSA and AMS NR amine fragments were moderate ($R = 0.50$) in Late Spring and strong ($R = 0.90$) in Autumn, indicating that AMS NR amine fragments during marine periods likely included a secondary marine source. IC MSA measurements were below detection during Winter and too few marine air masses were sampled in Early Spring to be able to identify a correlation with any IC inorganic ions. Submicron FTIR NV amine groups were also moderately correlated ($R = 0.74$) with IC MSA for marine air masses in Late Spring supporting a secondary contribution to the FTIR NV amine groups as well. However, correlations with IC MSA of both FTIR NV and AMS NR amine were not significant ($p \geq 0.05$) due to the limited number of simultaneous IC filters available, which indicates that secondary marine source contributions to submicron mass are minor. Additional evidence for secondary contributions of FTIR NV amine groups is considered for <0.5 µm particles in Section 4.3.

4.2 Continental Amine Sources

Anthropogenic nitrogen oxides (NOx) can undergo a variety of reactions that form nitrate-containing secondary organic aerosols. For example, heterogeneous hydrolysis of dinitrogen pentoxide (N_2O_5) can produce nitric acid (HNO_3) that may form aminium nitrate salts though acid-base reactions with amines (Murphy et al., 2007;Price et al., 2016). Aminium salts can also

form by the displacement of ammonium by amine in ammonium nitrate. The volatility of these amine-containing compounds is lower than ammonium nitrate such that they are more likely to partition into the particle phase (Smith et al., 2010). The moderate to strong (0.67 < R < 0.84, Figure 5b) correlations of AMS NR amine fragments and AMS NR nitrate for the Winter,

295 Late Spring, and Autumn cruises during continental periods provide some evidence that the formation of particle-phase amine is associated with nitrate. To a lesser extent, AMS NR amine fragments and AMS NR nitrate also correlated weakly to moderately (0.31 < R < 0.79, Figure 5a) during the marine periods for the Winter, Late Spring, and Autumn cruises. This suggests a secondary continental source for AMS NR amine fragments that is present during continental and marine periods. Tables S17 and S18 contain the linear fits for AMS NR amine fragments and FTIR NV amine groups, respectively. The zero

300 intercepts (Table S17) of the linear fits for both continental air masses in Winter and Autumn and marine air masses in Winter and Late Spring suggest that the AMS NR amine fragments largely have continental sources that are present during clean marine periods at lower concentrations. Correlations for FTIR NV amine groups were not available for the continental periods in Autumn and the marine periods in Early Spring due to sampling limitations. No positive correlations (-0.59 < R < 0.19, p > 0.05) of FTIR NV amine groups and AMS NR nitrate were observed, suggesting that the aminium salts may not have primary

305 amine groups (CNH_2) or may be too volatile to remain for filter analysis.

Figures 6a and 6b shows the weak to strong (0.30 < R < 0.86) correlations of AMS NR amine fragments to black carbon for continental air masses as well as for Autumn marine air masses. This correlation is consistent with the correlation to AMS NR nitrate, as AMS NR nitrate and black carbon are typically produced by combustion. BC is often an indicator of a primary

310 combustion source, suggesting that AMS NR amine fragments may also include some primary sources of amines (Shen et al., 2017;Liu et al., 2022b). BC and AMS NR nitrate could be emitted by ocean-going vessels locally or transported from continents. Two tracers for continental processes are radon (from rocks and soils) and non-sea salt potassium (from biomass burning).

315 Since radon is a decay product of rocks and soil, it is used as a naturally occurring tracer for continental air masses. The weak correlation (R = 0.37, Figure 6c) of AMS NR amine fragments to radon during the marine period in Winter and moderate (0.55 < R < 0.66, Figure 6d) correlations during the continental periods in Winter, Autumn, and Late Spring indicate that much of the AMS NR amine fragments are continental. In contrast, all but the Late Spring marine period showed no or negative correlations (-0.67 < R < -0.01, Table 5) of FTIR NV amine groups with radon, suggesting that FTIR NV amine groups are

320 largely from marine sources. It is possible, however, for weaker correlations to arise from amines associated with secondary or urban emissions that are disproportionate to land-based emissions of radon.

Non-sea salt potassium (nssK$^+$) is a widely-used tracer for biomass burning, which also can produce a continental source of methylated amines (Bottenus et al., 2018). Weak to strong correlations (0.27 < R < 0.95, Figure 6e,f) of AMS NR amine

325 fragments to IC nssK$^+$ were found for all marine and continental periods when IC measurements of K$^+$ and sodium (Na$^+$) were

available. The correlations of AMS NR amine fragments and IC nssK$^+$ are significant for marine air masses in Winter and all continental seasons except Winter, suggesting an important continental contribution to AMS NR amine fragments. No correlations of FTIR NV amine groups to IC nssK$^+$ were statistically significant due to limited overlap of IC and FTIR filter sampling times (Table 5).

330

Ozone has also been used as a tracer for secondary processes when its availability has limited secondary aerosol formation (Liu et al., 2011;Verma et al., 2017). Some evidence for photochemical formation is observed by positive, weak correlations ($0.41 < R < 0.42$) during continental periods in Late Spring and Autumn (Figure 5d) but marine periods in Late and Early Spring and continental periods in Winter did not show positive correlations. The possible photochemical formation is supported

335 by the weak correlations with solar radiation during continental periods in Autumn ($R = 0.33$) and Early Spring ($R = 0.29$). FTIR NV amine groups weakly correlated ($0.28 < r < 0.48$, Table 5) with ozone during periods when no positive correlations ($-0.94 < R < 0.05$) with solar radiation were observed, providing inconsistent support for a photochemical contribution to FTIR NV amine groups.

340 The contribution of the AMS ion signal at m/z 44 (CO_2^+) to the total AMS NR OM signal (f_{44}) is a measure of particle oxidation and a tracer for secondary processing (Bahreini et al., 2005). Figures 5e and 5f display largely consistent trends between the contribution of AMS NR amine fragments to the AMS NR OM and f_{44}. Weak to moderate ($0.43 < R < 0.79$) correlations of AMS NR f_{44} and AMS NR amine fragments are present across all air masses and seasons. Murphy et al. (2007) identified large signals of AMS NR m/z 44 in mass spectra of aminium nitrate salts produced by photooxidation, providing further evidence

345 of secondary formation of AMS NR amine fragments. AMS NR f_{44} positively correlated ($R = 0.36$) with the contribution of FTIR NV amine group mass concentrations to the FTIR NV OM signal for only the marine period in Late Spring, possibly because aminium nitrate salts are too volatile to be retained on filters for FTIR analysis.

The Early Spring cruise began in Puerto Rico rather than Massachusetts and sampled marine air masses at latitudes lower than

350 the other cruises. Few sampled air masses in Early Spring met the criteria for "marine", in part because black carbon concentrations were high (29 ± 5 ng m^{-3}, Table 2) compared to other cruises. However, AMS NR amine fragments in Early Spring marine air masses did not correlate with continental tracers (black carbon, AMS NR nitrate, radon, or IC nssK$^+$). AMS NR amine fragments did correlate moderately with atmospheric DMS, ozone, and AMS NR f_{44}, which could be consistent with a secondary marine source that was not evident in the other cruises at higher latitudes. For marine air masses in Bermuda,

355 near where marine air masses were sampled in Early Spring, anthropogenic activity is not a large contributor to organic nitrogen compounds, such as amine, despite being downwind of continental pollution sources (Altieri et al., 2016). It is also possible that the lack of correlation with the available tracers could be from sampling shorter durations of marine air masses during Early Spring, which limits the comparison of Early Spring marine periods to marine periods in other seasons.

4.3 Sources for <0.5 and <0.18 µm Amines

360 Submicron (<1 µm) sampling of marine aerosol over the open ocean and from bubble generators has suggested that alcohol functional groups serve as useful tracers for marine-derived saccharides, amino sugars, and carbohydrates (Frossard et al., 2014a;Gagosian et al., 1982;Leck and Bigg, 2005;Russell et al., 2010;Lewis et al., 2021). Conversely, carboxylic acid groups serve as a tracer for photochemical reaction products of VOCs (Frossard et al., 2014a;Takahama et al., 2010;Russell et al., 2010;Liu et al., 2011;Claflin et al., 2021). Figure 7 shows the correlations of FTIR NV amine groups to FTIR NV alcohol

365 groups and FTIR NV acid groups measured across all four cruises for three different size cut-offs (<1 µm, <0.5 µm, <0.18 µm).

For FTIR NV alcohol and amine groups, <1 µm particle samples had a strong correlation (R = 0.87, Figure 7a) s for marine periods and a moderate correlation (R = 0.63, Figure 7b) for continental periods, consistent with a primary source of FTIR NV

370 amine groups. The difference between marine and continental air masses shows that the primary seawater amine source explains more variability for marine air masses than for continental air masses. The correlation of FTIR NV alcohol and amine groups was weaker for marine filters for <0.5 µm and <0.18 µm particle samples, with R = 0.31 for <0.5 µm (Figure 7c) and R = 0.11 for <0.18 µm (Figure 7e). Similarly, there were lower correlations of FTIR NV alcohol and amine groups for continental filters with R = 0.12 for <0.5 µm (Figure 7d) and R = 0.27 for <0.18 µm (Figure 7f). These results show that non-

375 volatile amine groups associated with sea spray are largely found in >0.5 µm particles, where their mass is sufficiently large to control the <1 µm mass variability. The weak correlations of FTIR NV alcohol and amine groups for <0.5 µm and <0.18 µm particle samples could result from non-marine sources such as combustion that have different ratios of FTIR NV alcohol and amine groups than those found in sea spray (Liu et al., 2009;Posner and Pandis, 2015;Shen et al., 2017;Liu et al., 2011). No positive correlations of <0.18 and <0.5 size fractions of FTIR NV amine group concentrations and black carbon

380 concentrations were observed for marine or continental air masses, indicating that primary combustion sources were not a major source of amine groups in these small size ranges.

In contrast to the strong correlations found for FTIR NV amine groups with FTIR NV alcohol group for <1 µm samples, no correlations of <1 µm FTIR NV amine to acid groups were found for either marine or continental air masses. The weak

385 correlations that were found for FTIR NV amine groups with FTIR NV alcohol groups for <0.5 µm and <0.18 µm particle samples also differ from the strong (0.82 < R < 0.96, Figure 7c,e) correlations of FTIR NV amine to acid groups that were found for <0.5 µm and <0.18 µm during marine periods. The correlations of FTIR NV acid to amine groups for <0.5 µm and <0.18 µm particle samples suggest that secondary amine groups contribute more to particles with diameters smaller than 0.5 µm, which is consistent with expectations for condensing gases having a proportionately larger impact on the mass composition

390 of smaller particles (Maria et al., 2004;Seinfeld and Pandis, 2016). Secondary dimethyl- and diethylaminium salts produced by acid-base reactions with biogenic, gaseous amines have been shown to have mass concentration peaks in similar size ranges

of 0.25-0.50 μm (Facchini et al., 2008) and 0.14-0.42 μm (Muller et al., 2009). The strong correlation between FTIR NV amine and acid groups for <0.5 μm and <0.18 μm particle samples indicate that a gas-to-particle reaction mechanism contributes to primary (C-NH$_2$) amine groups in size ranges that are important for CCN. A secondary marine source of FTIR NV amine groups in aerosols with diameters of <0.18 μm and <0.5 μm is supported by weak to moderate correlations ($0.39 < R < 0.73$) of MSA and FTIR NV amine groups during marine periods in Late Spring for both size ranges. There was no significant correlation between FTIR NV acid and amine groups for any size of the continental FTIR filters and too few continental filters with both FTIR NV amine and acid groups above detection to investigate correlations for continental <0.18 μm particle samples.

4.4 Combined AMS NR and FTIR NV Amine Contributions

In general, our results support the expectation that FTIR NV amine groups and AMS NR amine fragments do not measure the same chemical components. Specifically, FTIR measures NV amine groups with primary C-NH$_2$ groups that may or may not be refractory. The correlations summarized in Figure 8 show that, in marine air masses, most of the FTIR NV amine groups in <1 μm particles have sources that are primary and marine and that <0.5 μm and <0.18 μm diameter fractions have sources that are secondary and marine. In contrast, the AMS measures NR amine fragments with primary (C-NH$_2$), secondary (C$_2$-NH), and tertiary (C$_3$-N) amine moieties that may be too volatile to be sampled on filters, but the FTIR does not detect secondary (C$_2$-NH) and tertiary (C$_3$-N) amines even if they remain on filters. There is a 20% uncertainty associated with AMS and FTIR OM measurements (Russell et al., 2009a;Russell, 2003). A larger difference between the measurements is seen when there is substantial refractory material such as black carbon, mineral dust, and sea salt due to the reduced collection efficiency of the HR-ToF-AMS (Gilardoni et al., 2007) and when there is a high contribution of volatile components as in urban areas (Liu et al., 2009;Chen et al., 2018). The correlations summarized in Figure 8 illustrate that the correlations of the two measurement methods are not random, as might be expected if they are driven by detection limit issues. Specifically, the higher correlations of AMS NR amine fragments to continental and secondary tracers indicate the components measured are largely continental and secondary, although some contribution of primary source emissions from combustion and secondary marine emissions is also likely.

During marine periods in Late Spring, the variability of FTIR NV amine groups was largely explained by correlations with AMS NR chloride, IC sea salt, seawater DMS, and chl a, all of which are consistent with primary marine sources. In contrast, the variability of AMS NR amine fragments was largely explained by correlations with AMS NR nitrate, IC nssK$^+$, radon, and AMS NR f_{44}, all of which indicate continental secondary sources. Figure 9 shows similar correlations with AMS NR nitrate and chl a in marine air masses during Late Spring that exemplify the AMS NR amine fragments correlation to AMS NR nitrate concentrations and the FTIR NV amine groups correlation to chl a. A schematic diagram of amine sources, tracers, and amine-containing particle types in marine environments is shown in Figure S13.

The distinctly different sources of FTIR NV amine groups and AMS NR amine fragments suggest that combining the two measurements is likely to provide a better estimate of particle-phase amines in marine environments than either measurement separately. This approach is supported by the poor overall correlation of $\rho = 0.02$ (Figure 2a) of the two measurements. FTIR NV amine groups provide a good estimate of <1 µm amine group mass concentration with a primary marine source; AMS NR amine fragments provide a good estimate of continental amine sources that are likely secondary. Results for individual seasons illustrate that the contributions of FTIR NV amine groups and AMS NR amine fragments vary by season (based on Table 2). For Winter, FTIR NV primary (C-NH$_2$) amine groups from primary marine sources account for (53±76)% compared to (47±68)% secondary continental AMS NR amine fragments. For Late Spring and Autumn, FTIR NV primary (C-NH$_2$) amine groups from primary marine sources account for (34±37)% compared to (66±72)% secondary continental AMS NR amine fragments. For Early Spring, FTIR NV primary (C-NH$_2$) amine groups from primary marine sources account for (27±57)% compared to (73±152)% secondary continental AMS NR amine fragments.

5 Conclusions

FTIR and AMS amine measurements were used to investigate the sources of submicron aerosol in the North Atlantic during different seasons. Marine and continental air masses were distinguished to separate the different conditions that were measured. Amine concentrations from AMS and FTIR were compared to chemical and meteorological tracers for identification of marine and continental sources and primary and secondary processes. FTIR and AMS measured greater amine concentrations for continental air masses than for marine air masses except for the Early Spring cruise, likely due to its lower latitudes and less pristine marine air masses. AMS NR amine fragments largely correlated with secondary tracers such as AMS NR nitrate, ozone, AMS NR f_{44} , and IC MSA but did not correlate positively with seawater DMS, AMS NR chloride, chlorophyll a or wind speed. Correlations with tracers for secondary particles were lower for <1 µm FTIR NV amine groups than for AMS NR amine fragments, but correlations of FTIR NV amine groups with tracers of primary marine sources such as wind speed, IC sea salt, and seawater DMS, NR chloride, and chlorophyll a were higher than for AMS NR amine fragments.

FTIR NV amine groups measured during marine periods were found to have largely primary sources for <1 µm particles but secondary sources for <0.5 and <0.18 µm particles. Correlations with FTIR NV alcohol groups show the contribution of a primary source of non-volatile amine for aerosols with diameters <1 µm that had weaker correlations for <0.5 and <0.18 µm. Correlations between FTIR NV amine groups with both FTIR NV acid groups and IC MSA for particles <0.5 and <0.18 µm diameter revealed that secondary processes were a larger contributor for amine groups than in <1 µm particles.

Results presented herein are also consistent with the expectation that FTIR measures the refractory, amine-containing sea salt particles missed by AMS, and that AMS measures the semi-volatile, amine-containing particles missed by FTIR spectroscopy. Therefore, these two techniques offer complementary analyses of amine in marine environments for <1 µm atmospheric

particles. Combining them provides a rough source apportionment for marine periods, with amine from primary marine sources accounting for (53±76)% compared to (47±68)% secondary continental amine in Winter, but amine from primary marine sources accounting for only (27±57)% compared to (73±152)% secondary continental amine for Early Spring.

Acknowledgements

The authors would like to thank the dedicated officers and crew of the R/V Atlantis. The authors would also like to acknowledge Savannah Lewis, Eric Saltzman, Laura Rivellini, Bill Brooks, Tim Onasch, Leah Williams, Raghu Betha, Maryam Askari Lamjiri, Derek Coffman, and Lucia Upchurch for their contributions to collecting and reducing data. This work was funded by NASA NAAMES grant NNX15AE66G, and VB was supported by the UCSD McNair Fellowship Program. This is PMEL contribution number 5413.

Data Availability

All data collected during NAAMES are available on the NASA data server: https://naames.larc.nasa.gov. Scripps measurements: https://library.ucsd.edu/dc/collection/bb34508432; Shipboard measurements: https://seabass.gsfc.nasa.gov/. PMEL measurements: https://saga.pmel.noaa.gov/data/.

References

Altieri, K. E., Fawcett, S. E., Peters, A. J., Sigman, D. M., and Hastings, M. G.: Marine biogenic source of atmospheric organic nitrogen in the subtropical North Atlantic, Proceedings of the National Academy of Sciences of the United States of America, 113, 925-930, 10.1073/pnas.1516847113, 2016.

Bahreini, R., Keywood, M. D., Ng, N. L., Varutbangkul, V., Gao, S., Flagan, R. C., Seinfeld, J. H., Worsnop, D. R., and Jimenez, J. L.: Measurements of secondary organic aerosol from oxidation of cycloalkenes, terpenes, and m-xylene using an Aerodyne aerosol mass spectrometer, Environmental Science & Technology, 39, 5674-5688, 10.1021/es048061a, 2005.

Bates, T. S., Quinn, P. K., Frossard, A. A., Russell, L. M., Hakala, J., Petaja, T., Kulmala, M., Covert, D. S., Cappa, C. D., Li, S. M., Hayden, K. L., Nuaaman, I., McLaren, R., Massoli, P., Canagaratna, M. R., Onasch, T. B., Sueper, D., Worsnop, D. R., and Keene, W. C.: Measurements of ocean derived aerosol off the coast of California, Journal of Geophysical Research-Atmospheres, 117, 10.1029/2012jd017588, 2012.

Bates, T. S., Quinn, P. K., Coffman, D. J., Johnson, J. E., Upchurch, L., Saliba, G., Lewis, S., Graff, J., Russell, L. M., and Behrenfeld, M. J.: Variability in Marine Plankton Ecosystems Are Not Observed in Freshly Emitted Sea Spray Aerosol Over the North Atlantic Ocean, Geophysical Research Letters, 47, 10.1029/2019gl085938, 2020.

Beale, R., and Airs, R.: Quantification of glycine betaine, choline and trimethylamine N-oxide in seawater particulates: Minimisation of seawater associated ion suppression, Analytica Chimica Acta, 938, 114-122, 10.1016/j.aca.2016.07.016, 2016.

Behrenfeld, M. J., Moore, R. H., Hostetler, C. A., Graff, J., Gaube, P., Russell, L. M., Chen, G., Doney, S. C., Giovannoni, S., Liu, H. Y., Proctor, C., Bolalios, L. M., Baetge, N., Davie-Martin, C., Westberry, T. K., Bates, T. S., Bell, T. G., Bidle, K. D., Boss, E. S., Brooks, S. D., Cairns, B., Carlson, C., Halsey, K., Harvey, E. L., Hu, C. M., Karp-Boss, L., Kleb, M., Menden-Deuer, S., Morison, F., Quinn, P. K., Scarino, A. J., Anderson, B., Chowdhary, J., Crosbie, E., Ferrare, R., Haire, J. W., Hu, Y. X., Janz, S., Redemann, J., Saltzman, E., Shook, M., Siegel, D. A., Wisthaler, A., Martine, M. Y., and Ziemba, L.: The

North Atlantic Aerosol and Marine Ecosystem Study (NAAMES): Science Motive and Mission Overview, Frontiers in Marine Science, 6, 10.3389/fmars.2019.00122, 2019.

Bell, T. G., Porter, J. G., Wang, W. L., Lawler, M. J., Boss, E., Behrenfeld, M. J., and Saltzman, E. S.: Predictability of Seawater DMS During the North Atlantic Aerosol and Marine Ecosystem Study (NAAMES), Frontiers in Marine Science, 7, 10.3389/fmars.2020.596763, 2021.

Bork, N., Elm, J., Olenius, T., and Vehkamaki, H.: Methane sulfonic acid-enhanced formation of molecular clusters of sulfuric acid and dimethyl amine, Atmospheric Chemistry and Physics, 14, 12023-12030, 10.5194/acp-14-12023-2014, 2014.

Bottenus, C. L. H., Massoli, P., Sueper, D., Canagaratna, M. R., VanderSchelden, G., Jobson, B. T., and VanReken, T. M.: Identification of amines in wintertime ambient particulate material using high resolution aerosol mass spectrometry, Atmospheric Environment, 180, 173-183, 10.1016/j.atmosenv.2018.01.044, 2018.

Carlson, C. A., Ducklow, H. W., and Michaels, A. F.: ANNUAL FLUX OF DISSOLVED ORGANIC-CARBON FROM THE EUPHOTIC ZONE IN THE NORTHWESTERN SARGASSO SEA, Nature, 371, 405-408, 10.1038/371405a0, 1994.

Carpenter, L. J., Fleming, Z. L., Read, K. A., Lee, J. D., Moller, S. J., Hopkins, J. R., Purvis, R. M., Lewis, A. C., Muller, K., Heinold, B., Herrmann, H., Fomba, K. W., van Pinxteren, D., Muller, C., Tegen, I., Wiedensohler, A., Muller, T., Niedermeier, N., Achterberg, E. P., Patey, M. D., Kozlova, E. A., Heimann, M., Heard, D. E., Plane, J. M. C., Mahajan, A., Oetjen, H., Ingham, T., Stone, D., Whalley, L. K., Evans, M. J., Pilling, M. J., Leigh, R. J., Monks, P. S., Karunaharan, A., Vaughan, S., Arnold, S. R., Tschritter, J., Pohler, D., Friess, U., Holla, R., Mendes, L. M., Lopez, H., Faria, B., Manning, A. J., and Wallace, D. W. R.: Seasonal characteristics of tropical marine boundary layer air measured at the Cape Verde Atmospheric Observatory, Journal of Atmospheric Chemistry, 67, 87-140, 10.1007/s10874-011-9206-1, 2010.

Chen, C. L., Chen, S. J., Russell, L. M., Liu, J., Price, D. J., Betha, R., Sanchez, K. J., Lee, A. K. Y., Williams, L., Collier, S. C., Zhang, Q., Kumar, A., Kleeman, M. J., Zhang, X. L., and Cappa, C. D.: Organic Aerosol Particle Chemical Properties Associated With Residential Burning and Fog in Wintertime San Joaquin Valley (Fresno) and With Vehicle and Firework Emissions in Summertime South Coast Air Basin (Fontana), Journal of Geophysical Research-Atmospheres, 123, 10707-10731, 10.1029/2018jd028374, 2018.

Chen, H. H., Ezell, M. J., Arquero, K. D., Varner, M. E., Dawson, M. L., Gerber, R. B., and Finlayson-Pitts, B. J.: New particle formation and growth from methanesulfonic acid, trimethylamine and water, Physical Chemistry Chemical Physics, 17, 13699-13709, 10.1039/c5cp00838g, 2015.

Chen, H. H., Varner, M. E., Gerber, R. B., and Finlayson-Pitts, B. J.: Reactions of Methanesulfonic Acid with Amines and Ammonia as a Source of New Particles in Air, Journal of Physical Chemistry B, 120, 1526-1536, 10.1021/acs.jpcb.5b07433, 2016.

Chen, H. H., and Finlayson-Pitts, B. J.: New Particle Formation from Methanesulfonic Acid and Amines/Ammonia as a Function of Temperature, Environmental Science & Technology, 51, 243-252, 10.1021/acs.est.6b04173, 2017.

Claflin, M. S., Liu, J., Russell, L. M., and Ziemann, P. J.: Comparison of methods of functional group analysis using results from laboratory and field aerosol measurements, Aerosol Science and Technology, 55, 1042-1058, 10.1080/02786826.2021.1918325, 2021.

DeCarlo, P. F., Kimmel, J. R., Trimborn, A., Northway, M. J., Jayne, J. T., Aiken, A. C., Gonin, M., Fuhrer, K., Horvath, T., Docherty, K. S., Worsnop, D. R., and Jimenez, J. L.: Field-deployable, high-resolution, time-of-flight aerosol mass spectrometer, Analytical Chemistry, 78, 8281-8289, 10.1021/ac061249n, 2006.

Facchini, M. C., Decesari, S., Rinaldi, M., Carbone, C., Finessi, E., Mircea, M., Fuzzi, S., Moretti, F., Tagliavini, E., Ceburnis, D., and O'Dowd, C. D.: Important Source of Marine Secondary Organic Aerosol from Biogenic Amines, Environmental Science & Technology, 42, 9116-9121, 10.1021/es8018385, 2008.

Frossard, A. A., Russell, L. M., Burrows, S. M., Elliott, S. M., Bates, T. S., and Quinn, P. K.: Sources and composition of submicron organic mass in marine aerosol particles, Journal of Geophysical Research-Atmospheres, 119, 12977-13003, 10.1002/2014jd021913, 2014a.

Frossard, A. A., Russell, L. M., Massoli, P., Bates, T. S., and Quinn, P. K.: Side-by-Side Comparison of Four Techniques Explains the Apparent Differences in the Organic Composition of Generated and Ambient Marine Aerosol Particles, Aerosol Science and Technology, 48, V-X, 10.1080/02786826.2013.879979, 2014b.

Gagosian, R. B., Zafiriou, O. C., Peltzer, E. T., and Alford, J. B.: LIPIDS IN AEROSOLS FROM THE TROPICAL NORTH PACIFIC - TEMPORAL VARIABILITY, Journal of Geophysical Research-Oceans, 87, 1133-1144, 10.1029/JC087iC13p11133, 1982.

Ge, X., Wexler, A. S., and Clegg, S. L.: Atmospheric amines - Part I. A review, Atmospheric Environment, 45, 524-546, 2011.

Gilardoni, S., Russell, L. M., Sorooshian, A., Flagan, R. C., Seinfeld, J. H., Bates, T. S., Quinn, P. K., Allan, J. D., Williams, B., Goldstein, A. H., Onasch, T. B., and Worsnop, D. R.: Regional variation of organic functional groups in aerosol particles on four US east coast platforms during the International Consortium for Atmospheric Research on Transport and Transformation 2004 campaign, Journal of Geophysical Research-Atmospheres, 112, 10.1029/2006jd007737, 2007.

Hawkins, L. N., Russell, L. M., Covert, D. S., Quinn, P. K., and Bates, T. S.: Carboxylic acids, sulfates, and organosulfates in processed continental organic aerosol over the southeast Pacific Ocean during VOCALS-REx 2008, Journal of Geophysical Research-Atmospheres, 115, 16, 10.1029/2009jd013276, 2010.

Huang, X. F., Kao, S. J., Lin, J., Qin, X. F., and Deng, C. R.: Development and validation of a HPLC/FLD method combined with online derivatization for the simple and simultaneous determination of trace amino acids and alkyl amines in continental and marine aerosols, Plos One, 13, 10.1371/journal.pone.0206488, 2018.

Kamruzzaman, M., Takahama, S., and Dillner, A. M.: Quantification of amine functional groups and their influence on OM/OC in the IMPROVE network, Atmospheric Environment, 172, 124-132, 10.1016/j.atmosenv.2017.10.053, 2018.

Keller, M. D.: Dimethyl Sulfide Production and Marine Phytoplankton: The Importance of Species Composition and Cell Size, Biological Oceanography, 6, 375-382, 10.1080/01965581.1988.10749540, 1989.

King, G. M.: DISTRIBUTION AND METABOLISM OF QUATERNARY AMINES IN SALT MARSHES, Estuaries, 8, A6-A6, 1985.

Kollner, F., Schneider, J., Willis, M. D., Klimach, T., Helleis, F., Bozem, H., Kunkel, D., Hoor, P., Burkart, J., Leaitch, W. R., Aliabadi, A. A., Abbatt, J. P. D., Herber, A. B., and Borrmann, S.: Particulate trimethylamine in the summertime Canadian high Arctic lower troposphere, Atmospheric Chemistry and Physics, 17, 13747-13766, 10.5194/acp-17-13747-2017, 2017.

Leck, C., and Bigg, E. K.: Source and evolution of the marine aerosol - A new perspective, Geophysical Research Letters, 32, 10.1029/2005gl023651, 2005.

Lee, C.: Amino Acid and Amine Biogeochemistry in Marine Particulate Material and Sediments, in: Nitrogen Cycling in Coastal Marine Environments, Wiley, 1988.

Lewis, S., Russell, L., Saliba, G., Quinn, P., Bates, T., Carlson, C., Baetge, N., Aluwihare, L., Boss, E., Frossard, A., Bell, T., and Behrenfeld, M.: Characterization of Sea Surface Microlayer and Marine Aerosol Organic Composition Using STXM-NEXAFS Microscopy and FTIR Spectroscopy, ACS Earth and Space Chemistry, 10.1021/acsearthspacechem.2c00119, 2022.

Lewis, S. L., Saliba, G., Russell, L. M., Quinn, P. K., Bates, T. S., and Behrenfeld, M. J.: Seasonal Differences in Submicron Marine Aerosol Particle Organic Composition in the North Atlantic, Frontiers in Marine Science, 8, 13, 10.3389/fmars.2021.720208, 2021.

Liu, Q., Nishibori, N., and Hollibaugh, J. T.: Sources of polyamines in coastal waters and their links to phytoplankton, Marine Chemistry, 242, 10.1016/j.marchem.2022.104121, 2022a.

Liu, S., Takahama, S., Russell, L. M., Gilardoni, S., and Baumgardner, D.: Oxygenated organic functional groups and their sources in single and submicron organic particles in MILAGRO 2006 campaign, Atmospheric Chemistry and Physics, 9, 6849-6863, 2009.

Liu, S., Day, D. A., Shields, J. E., and Russell, L. M.: Ozone-driven daytime formation of secondary organic aerosol containing carboxylic acid groups and alkane groups, Atmospheric Chemistry and Physics, 11, 8321-8341, 10.5194/acp-11-8321-2011, 2011.

Liu, Z. Y., Li, M., Wang, X. F., Liang, Y. H., Jiang, Y. R., Chen, J., Mu, J. S., Zhu, Y. J., Meng, H., Yang, L. X., Hou, K. Y., Wang, Y. F., and Xue, L. K.: Large contributions of anthropogenic sources to amines in fine particles at a coastal area in northern China in winter, Science of the Total Environment, 839, 10.1016/j.scitotenv.2022.156281, 2022b.

Malin, G., Turner, S., Liss, P., Holligan, P., and Harbour, D.: DIMETHYLSULFIDE AND DIMETHYLSULPHONIOPROPIONATE IN THE NORTHEAST ATLANTIC DURING THE SUMMER COCCOLITHOPHORE BLOOM, Deep-Sea Research Part I-Oceanographic Research Papers, 40, 1487-1508, 10.1016/0967-0637(93)90125-m, 1993.

Malloy, Q. G. J., Qi, L., Warren, B., Cocker, D. R., Erupe, M. E., and Silva, P. J.: Secondary organic aerosol formation from primary aliphatic amines with NO3 radical, Atmospheric Chemistry and Physics, 9, 2051-2060, 10.5194/acp-9-2051-2009, 2009.

Maria, S. F., Russell, L. M., Turpin, B. J., and Porcja, R. J.: FTIR measurements of functional groups and organic mass in aerosol samples over the Caribbean, Atmospheric Environment, 36, 5185-5196, 10.1016/s1352-2310(02)00654-4, 2002.

Maria, S. F., Russell, L. M., Gilles, M. K., and Myneni, S. C. B.: Organic aerosol growth mechanisms and their climate-forcing implications, Science, 306, 1921-1924, 10.1126/science.1103491, 2004.

Mausz, M. A., and Chen, Y.: Microbiology and Ecology of Methylated Amine Metabolism in Marine Ecosystems, Current
595 Issues in Molecular Biology, 33, 133-148, 10.21775/cimb.033.133, 2019.

Miyazaki, Y., Kawamura, K., Jung, J., Furutani, H., and Uematsu, M.: Latitudinal distributions of organic nitrogen and organic carbon in marine aerosols over the western North Pacific, Atmospheric Chemistry and Physics, 11, 3037-3049, 10.5194/acp-11-3037-2011, 2011.

Muller, C., Iinuma, Y., Karstensen, J., van Pinxteren, D., Lehmann, S., Gnauk, T., and Herrmann, H.: Seasonal variation of
600 aliphatic amines in marine sub-micrometer particles at the Cape Verde islands, Atmospheric Chemistry and Physics, 9, 9587-9597, 2009.

Murphy, S. M., Sorooshian, A., Kroll, J. H., Ng, N. L., Chhabra, P., Tong, C., Surratt, J. D., Knipping, E., Flagan, R. C., and Seinfeld, J. H.: Secondary aerosol formation from atmospheric reactions of aliphatic amines, Atmospheric Chemistry and Physics, 7, 2313-2337, 10.5194/acp-7-2313-2007, 2007.

605 Myriokefalitakis, S., Vignati, E., Tsigaridis, K., Papadimas, C., Sciare, J., Mihalopoulos, N., Facchini, M. C., Rinaldi, M., Dentener, F. J., Ceburnis, D., Hatzianastasiou, N., O'Dowd, C. D., van Weele, M., and Kanakidou, M.: Global Modeling of the Oceanic Source of Organic Aerosols, Advances in Meteorology, 2010, 10.1155/2010/939171, 2010.

O'Dowd, C. D., Facchini, M. C., Cavalli, F., Ceburnis, D., Mircea, M., Decesari, S., Fuzzi, S., Yoon, Y. J., and Putaud, J. P.: Biogenically driven organic contribution to marine aerosol, Nature, 431, 676-680, 10.1038/nature02959, 2004.

610 Perraud, V. P., Xu, X., Gerber, R. B., and Finlayson-Pitts, B. J.: Integrated experimental and theoretical approach to probe the synergistic effect of ammonia in methanesulfonic acid reactions with small alkylamines, Environmental Science-Processes & Impacts, 22, 305-328, 10.1039/c9em00431a, 2020.

Pilson, M. E. Q.: An Introduction to the Chemistry of the Sea, Cambridge University press, 2013.

Posner, L. N., and Pandis, S. N.: Sources of ultrafine particles in the Eastern United States, Atmospheric Environment, 111,
615 103-112, 10.1016/j.atmosenv.2015.03.033, 2015.

Price, D. J., Kacarab, M., Cocker, D. R., Purvis-Roberts, K. L., and Silva, P. J.: Effects of temperature on the formation of secondary organic aerosol from amine precursors, Aerosol Science and Technology, 50, 1216-1226, 10.1080/02786826.2016.1236182, 2016.

Quinn, P. K., Coffman, D. J., Kapustin, V. N., Bates, T. S., and Covert, D. S.: Aerosol optical properties in the marine boundary
620 layer during the First Aerosol Characterization Experiment (ACE 1) and the underlying chemical and physical aerosol properties, Journal of Geophysical Research-Atmospheres, 103, 16547-16563, 10.1029/97jd02345, 1998.

Quinn, P. K., Bates, T. S., Coffman, D. J., Upchurch, L., Johnson, J. E., Moore, R., Ziemba, L., Bell, T. G., Saltzman, E. S., Graff, J., and Behrenfeld, M. J.: Seasonal Variations in Western North Atlantic Remote Marine Aerosol Properties, Journal of Geophysical Research-Atmospheres, 124, 14240-14261, 10.1029/2019jd031740, 2019.

625 Russell, L. M.: Aerosol organic-mass-to-organic-carbon ratio measurements, Abstracts of Papers of the American Chemical Society, 225, U817-U818, 2003.

Russell, L. M., Bahadur, R., Hawkins, L. N., Allan, J., Baumgardner, D., Quinn, P. K., and Bates, T. S.: Organic aerosol characterization by complementary measurements of chemical bonds and molecular fragments, Atmospheric Environment, 43, 6100-6105, 10.1016/j.atmosenv.2009.09.036, 2009a.

630 Russell, L. M., Takahama, S., Liu, S., Hawkins, L. N., Covert, D. S., Quinn, P. K., and Bates, T. S.: Oxygenated fraction and mass of organic aerosol from direct emission and atmospheric processing measured on the R/V Ronald Brown during TEXAQS/GoMACCS 2006, Journal of Geophysical Research-Atmospheres, 114, 15, 10.1029/2008jd011275, 2009b.

Russell, L. M., Hawkins, L. N., Frossard, A. A., Quinn, P. K., and Bates, T. S.: Carbohydrate-like composition of submicron atmospheric particles and their production from ocean bubble bursting, Proceedings of the National Academy of Sciences of
635 the United States of America, 107, 6652-6657, 10.1073/pnas.0908905107, 2010.

Russell, L. M., Bahadur, R., and Ziemann, P. J.: Identifying organic aerosol sources by comparing functional group composition in chamber and atmospheric particles, Proceedings of the National Academy of Sciences of the United States of America, 108, 3516-3521, 10.1073/pnas.1006461108, 2011.

Russell, L. M., Chen, C.-L., Betha, R., Price, D. J., and Lewis, S.: Aerosol Particle Chemical and Physical Measurements on
640 the 2015, 2016, 2017, and 2018 North Atlantic Aerosols and Marine Ecosystems Study (NAAMES) Research Cruises (Curated Collection). UC San Diego Library Digital Collections, in, UC San Diego Library Digital Collections, 2018.

Saliba, G., Chen, C. L., Lewis, S., Russell, L. M., Rivellini, L. H., Lee, A. K. Y., Quinn, P. K., Bates, T. S., Haentjens, N., Boss, E. S., Karp-Boss, L., Baetge, N., Carlson, C. A., and Behrenfeld, M. J.: Factors driving the seasonal and hourly variability of sea-spray aerosol number in the North Atlantic, Proceedings of the National Academy of Sciences of the United States of

645   America, 116, 20309-20314, 10.1073/pnas.1907574116, 2019.

Saliba, G., Chen, C. L., Lewis, S., Russell, L. M., Quinn, P. K., Bates, T. S., Bell, T. G., Lawler, M. J., Saltzman, E. S., Sanchez, K. J., Moore, R., Shook, M., Rivellini, L. H., Lee, A., Baetge, N., Carlson, C. A., and Behrenfeld, M. J.: Seasonal Differences and Variability of Concentrations, Chemical Composition, and Cloud Condensation Nuclei of Marine Aerosol Over the North Atlantic, Journal of Geophysical Research-Atmospheres, 125, 24, 10.1029/2020jd033145, 2020.

650   Sanchez, K. J., Chen, C. L., Russell, L. M., Betha, R., Liu, J., Price, D. J., Massoli, P., Ziemba, L. D., Crosbie, E. C., Moore, R. H., Muller, M., Schiller, S. A., Wisthaler, A., Lee, A. K. Y., Quinn, P. K., Bates, T. S., Porter, J., Bell, T. G., Saltzman, E. S., Vaillancourt, R. D., and Behrenfeld, M. J.: Substantial Seasonal Contribution of Observed Biogenic Sulfate Particles to Cloud Condensation Nuclei, Scientific Reports, 8, 10.1038/s41598-018-21590-9, 2018.

Schurman, M. I., Lee, T., Desyaterik, Y., Schichtel, B. A., Kreidenweis, S. M., and Collett, J. L.: Transport, biomass burning,
655   and in-situ formation contribute to fine particle concentrations at a remote site near Grand Teton National Park, Atmospheric Environment, 112, 257-268, 10.1016/j.atmosenv.2015.04.043, 2015.

Seinfeld, J. H., and Pandis, S. N.: Atmospheric Chemistry and Physics: From Air Pollution to Climate Change, 3rd ed., Wiley & Sons, 2016.

Shen, W. C., Ren, L. L., Zhao, Y., Zhou, L. Y., Dai, L., Ge, X. L., Kong, S. F., Yan, Q., Xu, H. H., Jiang, Y. J., He, J., Chen,
660   M. D., and Yu, H. A.: C1-C2 alkyl aminiums in urban aerosols: Insights from ambient and fuel combustion emission measurements in the Yangtze River Delta region of China, Environmental Pollution, 230, 12-21, 10.1016/j.envpol.2017.06.034, 2017.

Smith, J. N., Barsanti, K. C., Friedli, H. R., Ehn, M., Kulmala, M., Collins, D. R., Scheckman, J. H., Williams, B. J., and McMurry, P. H.: Observations of aminium salts in atmospheric nanoparticles and possible climatic implications, Proceedings
665   of the National Academy of Sciences of the United States of America, 107, 6634-6639, 10.1073/pnas.0912127107, 2010.

Steiner, M., and Hartmann, T.: OCCURENCE AND DISTRIBUTION OF VOLATILE AMINES IN MARINE ALGAE, Planta, 79, 113-&, 10.1007/bf00390154, 1968.

Takahama, S., Liu, S., and Russell, L. M.: Coatings and clusters of carboxylic acids in carbon-containing atmospheric particles from spectromicroscopy and their implications for cloud-nucleating and optical properties, Journal of Geophysical Research-
670   Atmospheres, 115, 10.1029/2009jd012622, 2010.

Takahama, S., Johnson, A., and Russell, L. M.: Quantification of Carboxylic and Carbonyl Functional Groups in Organic Aerosol Infrared Absorbance Spectra, Aerosol Science and Technology, 47, 310-325, 10.1080/02786826.2012.752065, 2013.

Tang, X., Price, D., Praske, E., Vu, D. N., Purvis-Roberts, K., Silva, P. J., Cocker, D. R., and Asa-Awuku, A.: Cloud condensation nuclei (CCN) activity of aliphatic amine secondary aerosol, Atmospheric Chemistry and Physics, 14, 5959-5967,
675   10.5194/acp-14-5959-2014, 2014.

Tang, X. C., Price, D., Praske, E., Lee, S. A., Shattuck, M. A., Purvis-Roberts, K., Silva, P. J., Asa-Awuku, A., and Cocker, D. R.: NO3 radical, OH radical and O-3-initiated secondary aerosol formation from aliphatic amines, Atmospheric Environment, 72, 105-112, 10.1016/j.atmosenv.2013.02.024, 2013.

Thamban, N. M., Lalchandani, V., Kumar, V., Mishra, S., Bhattu, D., Slowik, J. G., Prevot, A. S. H., Satish, R., Rastogi, N.,
680   and Tripathi, S. N.: Evolution of size and composition of fine particulate matter in the Delhi megacity during later winter, Atmospheric Environment, 267, 10.1016/j.atmosenv.2021.118752, 2021.

van Pinxteren, M., Fomba, K. W., van Pinxteren, D., Triesch, N., Hoffmann, E. H., Cree, C. H. L., Fitzsimons, M. F., von Tumpling, W., and Herrmann, H.: Aliphatic amines at the Cape Verde Atmospheric Observatory: Abundance, origins and sea-air fluxes, Atmospheric Environment, 203, 183-195, 10.1016/j.atmosenv.2019.02.011, 2019.

685   Verma, N., Satsangi, A., Lakhani, A., and Kumari, K. M.: Low Molecular Weight Monocarboxylic Acids in PM2.5 and PM10: Quantification, Seasonal Variation and Source Apportionment, Aerosol and Air Quality Research, 17, 485-498, 10.4209/aaqr.2016.05.0183, 2017.

Wang, Y. L., Zhang, J. W., Marcotte, A. R., Karl, M., Dye, C., and Herckes, P.: Fog chemistry at three sites in Norway, Atmospheric Research, 151, 72-81, 10.1016/j.atmosres.2014.04.016, 2015.

690   Werdell, P. J., Bailey, S., Fargion, G., Pietras, C., Knobelspiesse, K., Feldman, G., and McClain, C.: Unique data repository facilitates ocean color satellite validation, Eos, Transactions American Geophysical Union, 84, 377-387, https://doi.org/10.1029/2003EO380001, 2003.

     Xie, H., Feng, L. M., Hu, Q. J., Zhu, Y. J., Gao, H. W., Gao, Y., and Yao, X. H.: Concentration and size distribution of water-extracted dimethylaminium and trimethylaminium in atmospheric particles during nine campaigns - Implications for sources,

695   phase states and formation pathways, Science of the Total Environment, 631-632, 130-141, 10.1016/j.scitotenv.2018.02.303, 2018.

     Yao, L., Garmash, O., Bianchi, F., Zheng, J., Yan, C., Kontkanen, J., Junninen, H., Mazon, S. B., Ehn, M., Paasonen, P., Sipila, M., Wang, M. Y., Wang, X. K., Xiao, S., Chen, H. F., Lu, Y. Q., Zhang, B. W., Wang, D. F., Fu, Q. Y., Geng, F. H., Li, L., Wang, H. L., Qiao, L. P., Yang, X., Chen, J. M., Kerminen, V. M., Petaja, T., Worsnop, D. R., Kulmala, M., and Wang, L.:

700   Atmospheric new particle formation from sulfuric acid and amines in a Chinese megacity, Science, 361, 278-+, 10.1126/science.aao4839, 2018.

     Youn, J. S., Crosbie, E., Maudlin, L. C., Wang, Z., and Sorooshian, A.: Dimethylamine as a major alkyl amine species in particles and cloud water: Observations in semi-arid and coastal regions, Atmospheric Environment, 122, 250-258, 10.1016/j.atmosenv.2015.09.061, 2015.

705

Table 1: Summary of recent measurements of amine concentrations in marine regions.

Sampling Site and Season	Relevant Findings	Citation
Southeast Pacific during October-November	FTIR primary amine groups. The average mass concentration ($\mu g\ m^{-3}$) for campaign: 0.015 ± 0.014; marine air masses: 0.0089 ± 0.0068; mixed air masses: 0.019 ± 0.015; continental air masses: 0.023 ± 0.023.	(Hawkins et al., 2010)
Gulf of Mexico during August- September	FTIR primary amine groups with contributions from oil combustion and wood smoke. The average mass concentration ($\mu g\ m^{-3}$) for campaign: 0.25 ± 0.26; air masses over the Gulf: 0.10 ± 0.07; southerly continental air masses: 0.48 ± 0.33; northerly continental air masses: 0.16 ± 0.13.	(Russell et al., 2009b)
Western Atlantic during August	FTIR primary amine groups. 2% of OM in all ambient aerosols, 13% of OM in generated primary marine aerosols.	(Frossard et al., 2014b)
Tropical East Atlantic during November-January (May-June)	HPLC with ESI-IT-MS secondary marine aliphatic amines (pg m^{-3}). MA: 2-520 (0-30); DMA: 100-1400 (130-360); DEA: 90-760 (5-110).	(Muller et al., 2009)
Gulf of Maine during June-August	FTIR primary amine groups below detection.	(Gilardoni et al., 2007)
Eastern North Atlantic during high biological activity	IC secondary, marine dimethylammonium and diethylammonium salts (ng m^{-3}) in clean air masses: 4-13 and 7-24, respectively. Concentrations peaked in 0.25-0.5 μm size range. Monoalkylammonium, and trialkylammonium salt concentrations below detection.	(Facchini et al., 2008)
Coastal Ireland during low (high) biological activity	IC secondary, marine dimethylammonium and diethylammonium salts (ng m^{-3}): <1-8 (2-24) and <1-12 (4-32), respectively. Monoalkylammonium and trialkylammonium salt concentrations below detection.	(Facchini et al., 2008)
La Jolla in coastal California during August-October	FTIR primary amine groups average mass concentration $0.11 \pm 0.09\ \mu g\ m^{-3}$. 1% of combustion (3.0 $\mu g\ m^{-3}$) were amines. 3% of marine (0.97 $\mu g\ m^{-3}$) were amines.	(Liu et al., 2011)
Western North Pacific during August-September	TOC/TON analyzer secondary, marine DEA: <0.1 to 0.8 ng m^{-3}.	(Miyazaki et al., 2011)
Coastal Northern China during January-February (November-December)	UHPLC-MS amines (MA, DEA, DMA, PA, TMA, MEA, PYR, BA, DEA, MOR, AN, DPA, TEA, DBA, TPA) with averages ranging from 0.1 to 58.7 (0.1 to 86.3) ng m^{-3} from coal combustion activities, industrial emissions, vehicle exhaust, biomass burning, and agricultural and marine emissions.	(Liu et al., 2022b)
Coastal Norway during September-November	GC-MS and LC-MS nitrosamines and alkyl amines (nM) in fog. MEA: BDL-7.1; MA: 0.4-8.9; DMA: 130.3-255; DEA: 1.7-5.8. NDEA, NMOR, NDBA, and NPIP, EA were below detection.	(Wang et al., 2015)
Tropical East Atlantic (2-year average)	IC secondary, aliphatic amines (ng m^{-3}) scavenged in the gas phase by the particle phase. DMA: 5.6; MA: 0.2; DEA: 3.9 .	(van Pinxteren et al., 2019)
Coastal California during July-August	IC and ICP-MS secondary, marine DMA: 2.3-70.3 ng m^{-3}.	(Youn et al., 2015)

Location	Method / Measurement	Reference
East China Sea during June	IC secondary, marine aliphatic amines (nmol m^{-3}). DMA: 0.67 ± 0.21; TMA: 0.20 ± 0.11.	(Xie et al., 2018)
Coastal site near Yellow Sea during August	IC secondary, marine aliphatic amines (nmol m^{-3}). DMA: 0.62 ± 0.50; TMA: 0.15 ± 0.11.	(Xie et al., 2018)
Yellow Sea and Northwest Pacific during March-May	IC secondary, marine aliphatic amines (nmol m^{-3}). DMA: 0.28 ± 0.23; TMA: 0.22 ± 0.23.	(Xie et al., 2018)
Yellow Sea and Bohai Sea during [1]August-September [2]June-July [3]November	IC secondary, marine methylated amines (nmol m^{-3}). [1]DMA: 0.52 ± 0.28; TMA: 0.31 ± 0113. [2]DMA: 1.1 ± 0.47; TMA: 0.35 ± 0.13. [3]DMA: 0.41 ± 0.36; TMA: 0.53 ± 0.32.	(Xie et al., 2018)
High Arctic during July	Single particle laser ablation AMS TMA: 23% of particles 200-1000 nm in diameter.	(Kollner et al., 2017)
Tropical East Atlantic during Winter and Spring	HPLC/ESI-IT-MS aliphatic amines. DMA and DEA: 270 pg m^{-3} (Spring) to 830 pg m^{-3} (Winter).	(Carpenter et al., 2010)
North Atlantic during September, May-June, March-April, November	FTIR primary amine groups. 5-8% of OM in atmospheric primary marine aerosols, 5-12% of OM in generated primary marine aerosols.	(Lewis et al., 2021)
California coast during May	FTIR primary amine groups. 14% of OM in generated primary marine aerosols.	(Bates et al., 2012)
Huaniao Island during January	HPLC/fluorescence alkyl amines (ng m^{-3}). MA: 0.27-7.04; EA: 0.37-1.78; PA: 0.76-4.03; BA: BDL-0.15; PEN: 0.07–0.40, HEX: BDL; MEA: 0.84–5.62.	(Huang et al., 2018)

[*]Abbreviations: MA- monomethylamine, DMA- dimethylamine, DEA- diethylamine, TMA- trimethylamine, EA-ethylamine, TEA-triethylamine, PA- propylamine. DPA- dipropylamine, TPA- tripropylamine, BA- butylamine, DBA - dibutylamine, MEA- ethanolamine, MOR-morpholine, PYR- pyrrolidine, AN- aniline, PEN- pentylamine, HEX- hexylamine, PIP- piperidine, NDMA-nitrosodimethylamine, NDEA-nitrosodiethylamine; NBA-nitrosodibutylamine; NPIP- nitrosopiperidine, UHPLC: Ultra High Performance Liquid Chromatography, GC: Gas Chromatography, ESI-IT-MS: Electrospray Ionization Ion Trap Mass Spectrometer, ICP: Inductively Coupled Plasma, TOC/TON: Total Organic Carbon/Total Organic Nitrogen

710

Table 2: Mean concentrations and standard deviations of amine, tracer, and environmental measurements during NAAMES for marine (first row) and continental (second row, in parentheses) periods. Seasonal mean concentrations and standard deviations are given in in square brackets, which were averaged over the sampling times of filters categorized as marine, continental, or mixed.

Season	Winter	Early Spring	Late Spring	Autumn
AMS NR Amine Fragments (ng/m^3)	14 ± 3 (18 ± 7) [18 ± 6]	33 ± 6 (32 ± 11) [31 ± 6]	23 ± 8 (37 ± 13) [33 ± 12]	26 ± 9 (54 ± 49) [30 ± 11]
FTIR NV Amine Groups (ng/m^3)*	10 ± 15 (33 ± 33) [20 ± 26]	BDL (16 ± 28) [12 ± 23]	18 ± 15 (21 ± 20) [17 ± 14]	7 ± 11 (28 ± 6) [16 ± 15]
Sum of AMS NR Amine Fragments & FTIR NV Amine Groups (ng/m^3)*	24 ± 15 (57 ± 31) [39 ± 27]	32 ± 7 (47 ± 30) [43 ± 25]	43 ± 14 (63 ± 15) [50 ± 16]	36 ± 16 (80 ± 10) [46 ± 21]
AMS NR OM (ng/m^3)	151 ± 47 (321 ± 309)	296 ± 107 (422 ± 227)	373 ± 269 (824 ± 658)	295 ± 150 (990 ± 1187)
FTIR NV OM (ng/m^3)	281 ± 198 (315 ± 220)	210 ± 156 (209 ± 327)	220 ± 165 (422 ± 420)	200 ± 175 (375 ± 431)
AMS NR Nitrate (ng/m^3)	6 ± 3 (12 ± 12)	9 ± 4 (15 ± 5)	10 ± 6 (45 ± 101)	8 ± 2 (14 ± 14)
AMS NR f_{44} (unitless)	0.39 ± 0.06 (0.35 ± 0.08)	0.50 ± 0.09 (0.49 ± 0.08)	0.38 ± 0.08 (0.31 ± 0.07)	0.56 ± 0.19 (0.45 ± 0.15)
Black Carbon (ng/m^3)	12 ± 14 (220 ± 354)	29 ± 5 (197 ± 62)	21 ± 16 (141 ± 240)	20 ± 17 (148 ± 147)
Ozone (ppb)	41 ± 2 (38 ± 5)	33 ± 14 (47 ± 9)	38 ± 7 (39 ± 6)	29 ± 6 (31 ± 7)
Radon (mBq/m^3)	246 ± 109 (472 ± 366)	272 ± 130 (873 ± 333)	298 ± 80 (466 ± 289)	404 ± 202 (876 ± 612)
Wind Speed (m/s)	9.9 ± 3.9 (10.4 ± 3.9)	9.2 ± 3.2 (11.7 ± 4.6)	9.7 ± 5.1 (6.6 ± 3.2)	9.4 ± 4.1 (5.9 ± 3.1)
atm. DMS (ppt)	66 ± 21 (93 ± 51)	129 ± 71 (91 ± 78)	463 ± 293 (214 ± 186)	138 ± 233 (118 ± 87)
sw. DMS (nmol/L)	1.4 ± 0.6 (1.4 ± 0.7)	3.0 ± 1.1 (4.6 ± 3.2)	3.2 ± 2.5 (2.5 ± 2.5)	3.3 ± 0.7 (3.1 ± 1.4)
Temperature (ºC)	10.2 ± 5.8 (11.9 ± 6.5)	19.7 ± 4.3 (13.6 ± 4.5)	8.5 ± 4.3 (9.1 ± 3.8)	13.5 ± 3.4 (16.7 ± 3.1)
Chlorophyll a (ng/L)	457 ± 242 (713 ± 774)	643 ± 247 (578 ± 360)	1956 ± 1689 (1647 ± 1396)	379 ± 236 (284 ± 255)
SST (ºC)	13.2 ± 0.5 (13.8 ± 5.5)	21.6 ± 3.6 (16.0 ± 3.2)	10.1 ± 5.1 (10.5 ± 4.7)	14.5 ± 2.8 (17.8 ± 4.2)
IC MSA (µg/m^3)	-- --	-- (0.11 ± 0.19)	0.05 ± 0.05 (0.06 ± 0.03)	0.01 ± 0.01 (0.01 ± 0.00)
IC Sea Salt (µg/m^3)	1.01 ± 0.75 (1.45 ± 0.72)	-- (1.28 ± 0.51)	0.30 ± 0.30 (0.06 ± 0.04)	0.45 ± 0.30 (0.43 ± 0.55)
IC nssK$^+$ (µg/m^3)	0.01 ± 0.01 (0.02 ± 0.01)	-- (0.02 ± 0.02)	0.00 ± 0.00 (0.02 ± 0.01)	0.00 ± 0.00 (0.03 ± 0.02)

*The average included filters with amine concentration below detection.

Table 3: Median concentrations and median absolute deviations of amine, tracer, and environmental measurements during NAAMES for marine (first row) and continental (second row, in parentheses) periods. Seasonal median concentrations and median absolute deviations are given in square brackets, which were averaged over the sampling times of filters categorized as marine, continental, or mixed.

Season	Winter	Early Spring	Late Spring	Autumn
AMS NR Amine Fragments (ng/m^3)	13 ± 2 (17 ± 5) [18 ± 4]	33 ± 5 (30 ± 7) [30 ± 4]	21 ± 6 (34 ± 12) [27 ± 10]	23 ± 7 (32 ± 33) [26 ± 9]
FTIR NV Amine Groups (ng/m^3)[*]	1 ± 12 (29 ± 25) [13 ± 20]	BDL (4 ± 19) [1 ± 25]	15 ± 12 (22 ± 13) [14 ± 11]	0 ± 10 (28 ±47) [17 ± 13]
Sum of AMS NR Amine Fragments & FTIR NV Amine Groups (ng/m^3)[*]	18 ± 11 (50 ± 24) [32 ± 21]	32 ± 5 (34 ± 22) [34 ± 17]	42 ± 11 (57 ± 12) [48 ± 13]	35 ± 12 (80 ± 7) [40 ± 17]
AMS NR OM (ng/m^3)	136 ± 38 (204 ± 205)	271 ± 61 (375 ± 142)	299 ± 151 (623 ± 403)	247 ± 114 (480 ± 806)
FTIR NV OM (ng/m^3)	260 ± 135 (295 ± 172)	210 ± 110 (80 ± 208)	180 ± 143 (260 ± 299)	145 ± 133 (375 ± 305)
AMS NR Nitrate (ng/m^3)	6 ± 2 (9 ± 7)	8 ± 2 (15 ± 4)	9 ± 3 (16 ± 49)	8 ± 2 (10 ± 8)
AMS NR f_{44} (unitless)	0.39 ± 0.45 (0.36 ± 0.06)	0.50 ± 0.06 (0.49 ± 0.06)	0.39 ± 0.06 (0.33 ± 0.06)	0.57 ± 0.13 (0.43 ± 0.11)
Black Carbon (ng/m^3)	6 ± 11 (74 ± 24)	23 ± 19 (120 ± 159)	15 ± 15 (77 ± 113)	16 ± 37 (76 ± 121)
Ozone (ppb)	41 ± 2 (39 ± 4)	27 ± 13 (50 ± 7)	40 ± 6 (39 ± 5)	30 ± 5 (34 ± 6)
Radon (mBq/m^3)	219 ± 78 (308 ± 281)	253 ± 80 (914 ± 253)	282 ± 61 (383 ± 191)	358 ± 202 (735 ± 460)
Wind Speed (m/s)	10.1 ± 3.3 (10.2 ± 3.1)	9.4 ± 2.7 (11.9 ± 3.5)	8.9 ± 4.0 (6.2 ± 2.3)	9.0 ± 3.1 (5.8 ± 2.5)
atm. DMS (ppt)	63 ± 15 75 ± 40)	134 ± 58 (68 ± 53)	373 ± 220 (173 ± 149)	63 ± 119 (98 ± 62)
sw. DMS (nmol/L)	1.3 ± 0.4 (1.2 ± 0.5)	2.7 ± 0.8 (3.7 ± 2.6)	2.4 ± 1.9 (1.56 ± 1.9)	3.3 ± 0.5 (2.7 ± 0.9)
Temperature (ºC)	10.2 ± 5.2 (13.9 ± 5.9)	22.1 ± 4.1 (12.6 ± 3.5)	7.7 ± 3.8 (9.1 ± 3.2)	12.6 ± 3.0 (17.2 ± 2.3)
Chlorophyll a (ng/L)	396 ± 180 (457 ± 519)	642 ± 206 (489 ± 259)	1246 ± 1267 (1212 ± 1098)	282 ± 210 (133 ± 219)
SST (ºC)	15.2 ± 4.7 (16.2 ± 4.9)	21.4 ± 3.3 (16.4 ± 2.4)	9.0 ± 4.7 (10.0 ± 4.1)	14.1 ± 2.2 (18.2 ± 3.4)
IC MSA (µg/m^3)	-- --	-- (0.00 ± 0.15)	0.03 ± 0.04 (0.06 ± 0.02)	0.01 ± 0.01 (0.01 ± 0.00)
IC Sea Salt (µg/m^3)	0.90 ± 0.55 (1.23 ± 0.53)	-- (1.26 ± 0.42)	0.14 ± 0.22 (0.05 ± 0.03)	0.44 ± 0.25 (0.23 ± 0.37)
IC nssK$^+$ (µg/m^3)	0.00 ± 0.01 (0.02 ± 0.01)	-- (0.01 ± 0.01)	0.00 ± 0.00 (0.02 ± 0.01)	0.00 ± 0.00 (0.02 ± 0.02)

Table 4: Pearson correlation (R) coefficient values between AMS NR amine fragments and various tracers for marine periods (columns 1-4) and continental periods (columns 5-8). Negative correlations are shaded blue and positive correlations are shaded red. The strength of each correlation determines the level of saturation for the corresponding shading- no correlation ($|R| < 0.25$)- gray, weak correlation ($0.25 \leq |R| < 0.50$)- light blue/red, moderate correlation ($0.50 \leq |R| < 0.80$)- medium blue/red, strong correlation ($0.80 \leq |R|$)- dark blue/red. Correlations that are not statistically significant ($p \geq 0.05$) are indicated by *.

Air Masses	Marine				Continental			
Season	Winter	Early Spring	Late Spring	Autumn	Winter	Early Spring	Late Spring	Autumn
AMS NR OM	0.85	0.27	0.80	0.78	0.73	0.83	0.81	0.98
FTIR NV OM	-0.26*	--	-0.07*	0.88*	-0.32*	0.48*	0.45*	--
AMS NR Nitrate	0.59	-0.17	0.79	0.31	0.71	0.10*	0.67*	0.84
AMS NR Sulfate	0.59	0.68	0.52	0.27	0.49	0.14	0.46	0.36
AMS NR Chloride	0.13	-0.09*	-0.08*	-0.07*	0.06*	-0.15	-0.07*	-0.03*
AMS NR f_{44}	0.46	0.43	0.68	0.79	0.85	0.51	0.76	0.76
Black Carbon	0.60*	-0.04*	0.61*	0.33	0.31	0.30	0.30*	0.86
Ozone	0.11*	-0.70	-0.25	-0.22	-0.26	0.02*	0.42	0.41
Radon	0.37	-0.01	-0.17*	0.03	0.66	0.18	0.55*	0.55
Wind Speed	-0.18	-0.09	-0.53*	0.03*	0.00	-0.41	-0.13*	-0.45
sw. DMS	0.08*	-0.06*	-0.09*	0.05*	0.07*	0.05*	-0.23*	-0.08
atm. DMS	-0.20	0.50	-0.20*	0.04	0.41	-0.34	-0.20	0.36
Solar Radiation	-0.03*	0.00*	0.16	0.08*	-0.02*	0.29	-0.05*	0.33
Relative Humidity	-0.55	0.00	-0.08*	-0.04*	0.11*	-0.26	0.04*	-0.49*
Temperature	-0.30	0.77	-0.17	0.34	0.21	0.26	0.41	0.59
Chlorophyll a	-0.09*	0.09	0.09	-0.46*	0.21*	-0.07*	-0.01*	-0.26*
SST	-0.15	0.80	-0.23	0.33	0.23	0.29	0.23	0.60
IC MSA	BDL	--	0.50*	0.90*	BDL	0.25*	0.12*	-0.10*
IC Sea Salt	0.59*	--	-0.72*	0.65*	-0.84*	0.15*	-0.17*	-0.05*
IC nssK$^+$	0.78	--	0.27*	0.83*	0.79*	0.59*	0.95	0.89

Table 5: Pearson correlation (R) coefficient values between FTIR NV amine groups (ADL & BDL) in particles with diameters <1 μm and various tracers for marine periods (columns 1-4) and continental periods (columns 5-8). Negative correlations are shaded blue and positive correlations are shaded red. The strength of each correlation determines the level of saturation for the corresponding shading- no correlation ($|R| < 0.25$)- gray, weak correlation ($0.25 \leq |R| < 0.50$)- light blue/red, moderate correlation ($0.50 \leq |R| < 0.80$)- medium blue/red, strong correlation ($0.80 \leq |R|$)- dark blue/red. Correlations that are not statistically significant ($p \geq 0.05$) are indicated by *.

Air Masses	Marine				Continental			
Season	Winter	Early Spring	Late Spring	Autumn	Winter	Early Spring	Late Spring	Autumn
AMS NR OM	-0.13*	--	0.26*	-0.14*	0.26*	0.54*	-0.66*	--
FTIR NV OM	0.68	--	0.90	0.69*	0.69	0.96	0.10*	--
AMS NR Nitrate	-0.16*	--	0.19*	-0.23*	0.01*	0.13*	-0.59*	--
AMS NR Sulfate	-0.19*	--	0.61*	0.27*	0.35*	-0.34*	-0.50*	--
AMS NR Chloride	0.57*	--	0.73*	0.00*	0.67	0.76	-0.43*	--
AMS NR f_{44}	0.03*	--	0.36*	0.00*	-0.54*	-0.67*	0.03*	--
Black Carbon	-0.16*	--	-0.84	0.14*	0.61*	0.04*	-0.26*	--
Ozone	0.45*	--	0.16*	-0.20*	0.17*	0.28*	0.31*	--
Radon	-0.67	--	0.28*	-0.23*	-0.54*	-0.01*	-0.32*	--
Wind Speed	-0.23*	--	-0.16*	0.04*	0.49*	0.52*	0.02*	--
sw. DMS	-0.30*	--	0.85*	-0.36*	0.54*	-0.26*	--	--
atm. DMS	-0.50*	--	0.46*	-0.15*	0.24*	0.05*	--	--
Solar Radiation	-0.43*	--	0.17*	-0.44*	0.49*	0.05*	-0.94*	--
Relative Humidity	-0.24*	--	0.77*	-0.01*	-0.21*	-0.45*	-0.74*	--
Temperature	-0.25*	--	-0.66*	0.32*	0.08*	-0.05*	-0.14*	--
Chlorophyll a	0.24*	--	0.86	-0.33*	-0.36*	0.09*	-0.26*	--
SST	-0.34*	--	-0.70*	0.66*	-0.31*	0.17*	0.02*	--
IC MSA	--	--	0.74*	-0.44*	--	-0.34*	-0.75*	--
IC Sea Salt	0.23*	--	0.33*	0.64*	--	0.78*	-0.25*	--
IC nssK^{+}	0.20*	--	0.35*	0.06*	--	0.72*	-0.31*	--
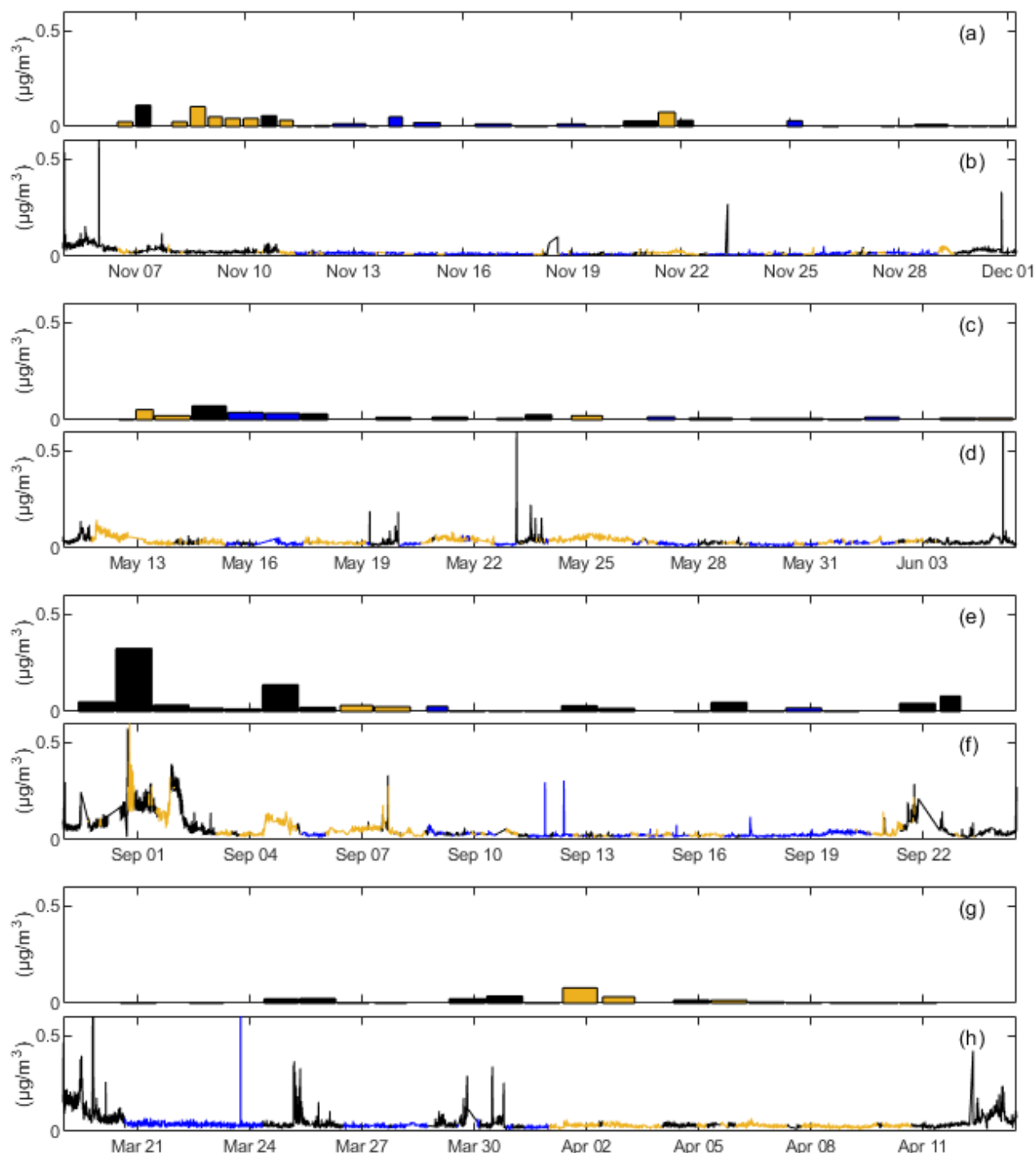
Figure 1: Time series of AMS NR amine fragments measured by the HR-ToF-AMS (b,d,f,h) and FTIR NV amine groups measured by FTIR spectroscopy in particles with diameters <1 μm (a,c,e,g) for all four cruises. From top to bottom: Winter (a,b), Late Spring (c,d), Autumn (e,f), Early Spring (g,h). Marker colors represent air mass type- blue: marine, yellow: continental, black: winds abaft or mixed.
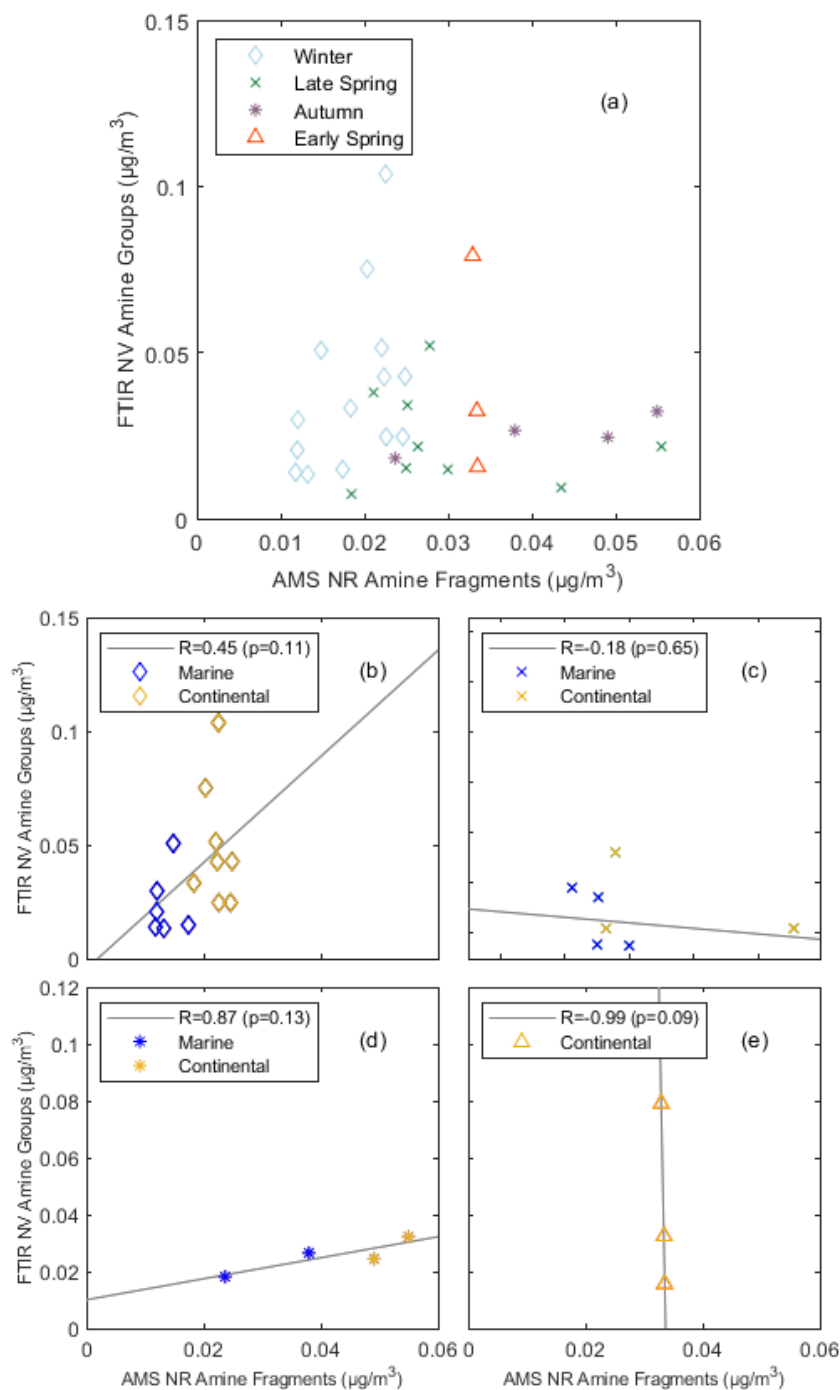
Figure 2: Scatter plot of (ADL) FTIR NV amine groups in particles with diameters <1 μm versus AMS NR amine fragments for (a) all cruises (ρ = 0.02, p = 0.18), (b) Winter, (c) Late Spring, (d) Autumn, and (e) Early Spring. Markers represent each cruise- open diamond: Winter, crosses: Late Spring, asterisk: Autumn, open triangle: Early Spring. Marker colors represent air mass type: blue: marine, yellow: continental. The solid grey lines are the lines of best fit obtained using an ordinary least squares regression. A two-tailed T test is used to estimate p-values.
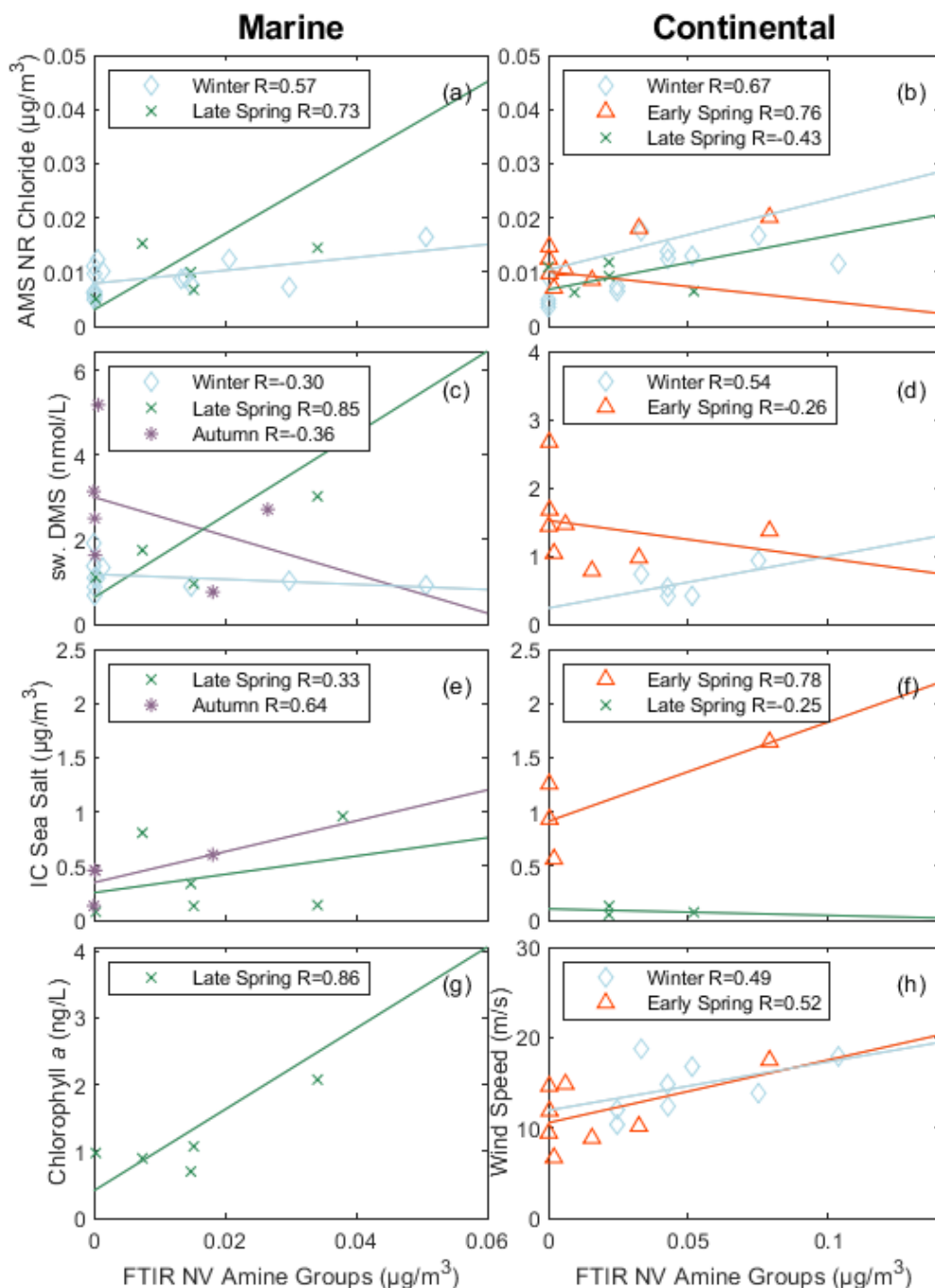
Figure 3: Scatter plot of marine tracers versus FTIR NV amine groups in particles with diameters <1 µm for marine periods (a,c,e,g) and continental periods (b,d,f,h). The panels include AMS NR chloride (a,b), seawater DMS (c,d), IC sea salt (e,f), chlorophyll *a* (g), wind speed (h). Markers represent each cruise- blue open diamond: Winter, green cross: Late Spring, purple asterisk: Autumn, red open triangle: Early Spring. The solid lines are the lines of best fit obtained using an ordinary least squares regression for |R| ≥ 0.25 with the exception of chlorophyll *a* which displays a fit only for R ≥ 0.25.

765
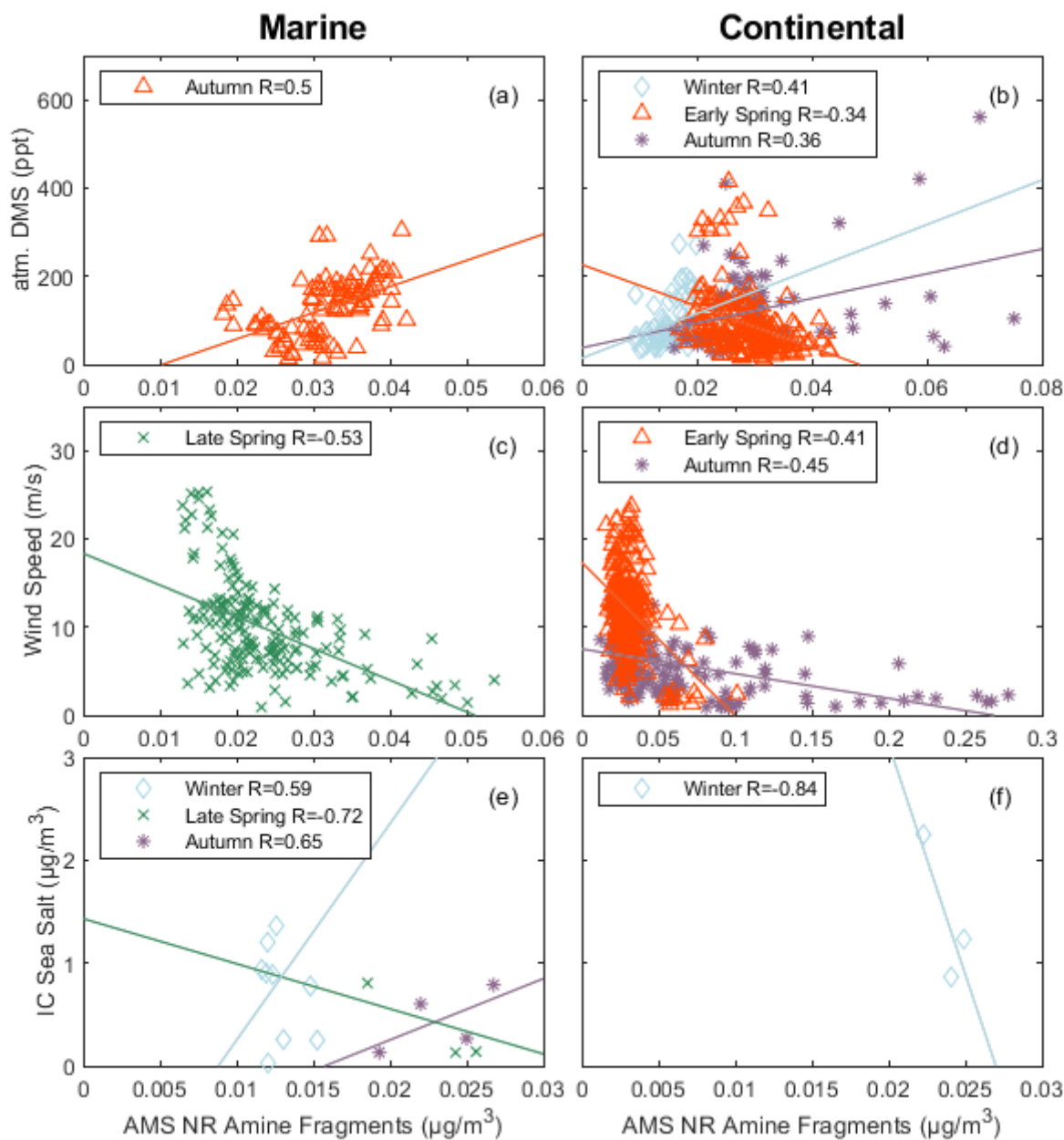
770 **Figure 4: Scatter plot of marine tracers versus AMS NR amine fragments for marine periods (a,c,e) and continental periods (b,d,f). The panels include atmospheric DMS (a,b), wind speed (c,d), IC sea salt (e,f). Markers represent each cruise- blue open diamond: Winter, green cross: Late Spring, purple asterisk: Autumn, red open triangle: Early Spring. The solid lines are the lines of best fit obtained using an ordinary least squares regression for R| ≥ 0.25.**
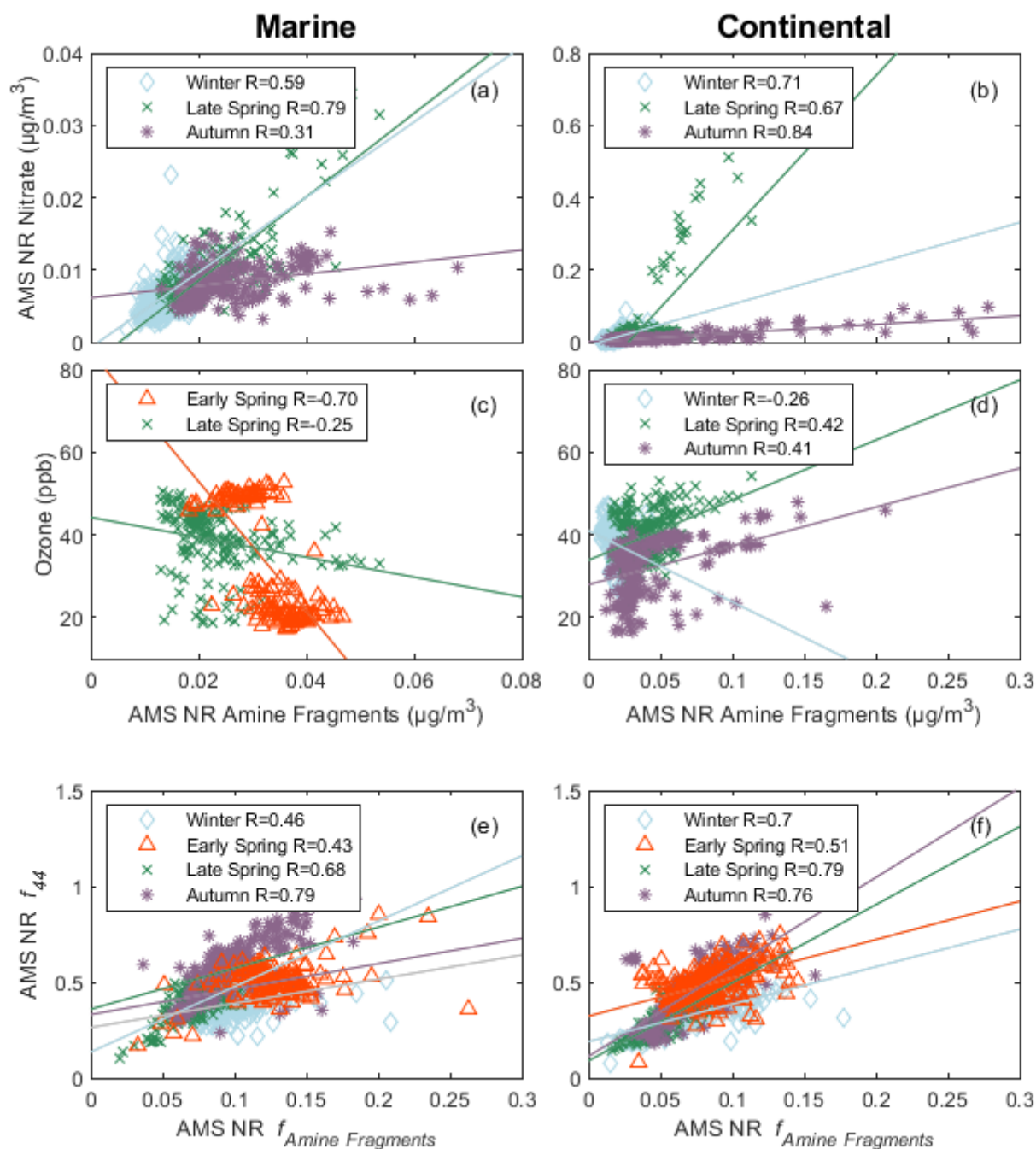
Figure 5: Scatter plot of secondary tracers versus AMS NR amine fragments for marine periods (a,c,e) and continental periods (b,d,f). The panels include submicron AMS NR nitrate (a,b), ozone (c,d), and AMS NR m/z 44 (e,f). Markers represent each cruise-blue open diamond: Winter, green cross: Late Spring, purple asterisk: Autumn, red open triangle: Early Spring. The solid lines are the lines of best fit obtained using an ordinary least squares regression for R| ≥ 0.25.
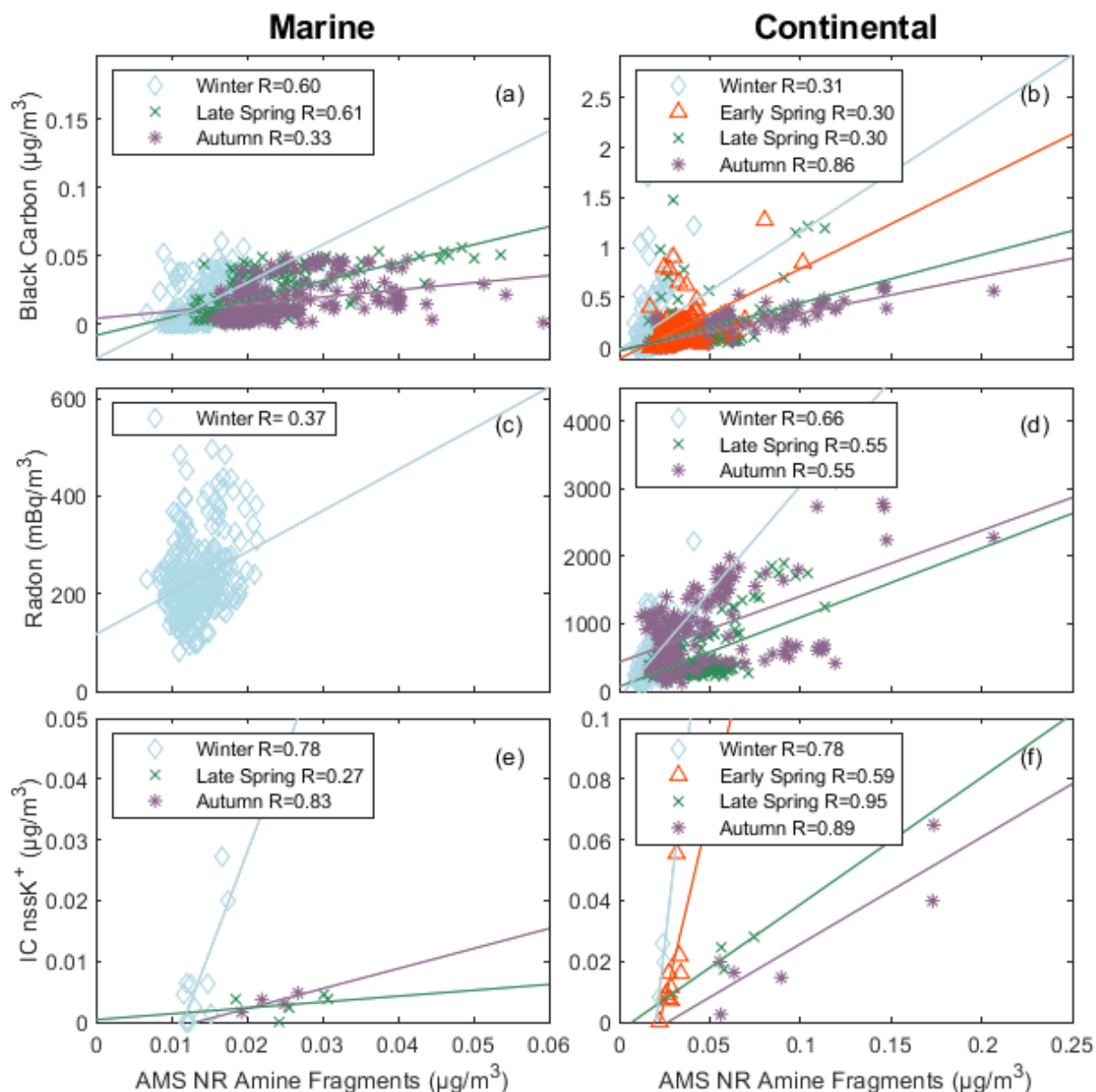
780 **Figure 6: Scatter plot of non-marine tracers versus AMS NR amine fragments for marine periods (a,c,e) and continental periods (b,d,f). The panels include black carbon (a,b), radon (c,d), IC nssK+ (e,f). Markers represent each cruise- blue open diamond: Winter, green cross: Late Spring, purple asterisk: Autumn, red open triangle: Early Spring. The solid lines are the lines of best fit obtained using an ordinary least squares regression for R| ≥ 0.25.**
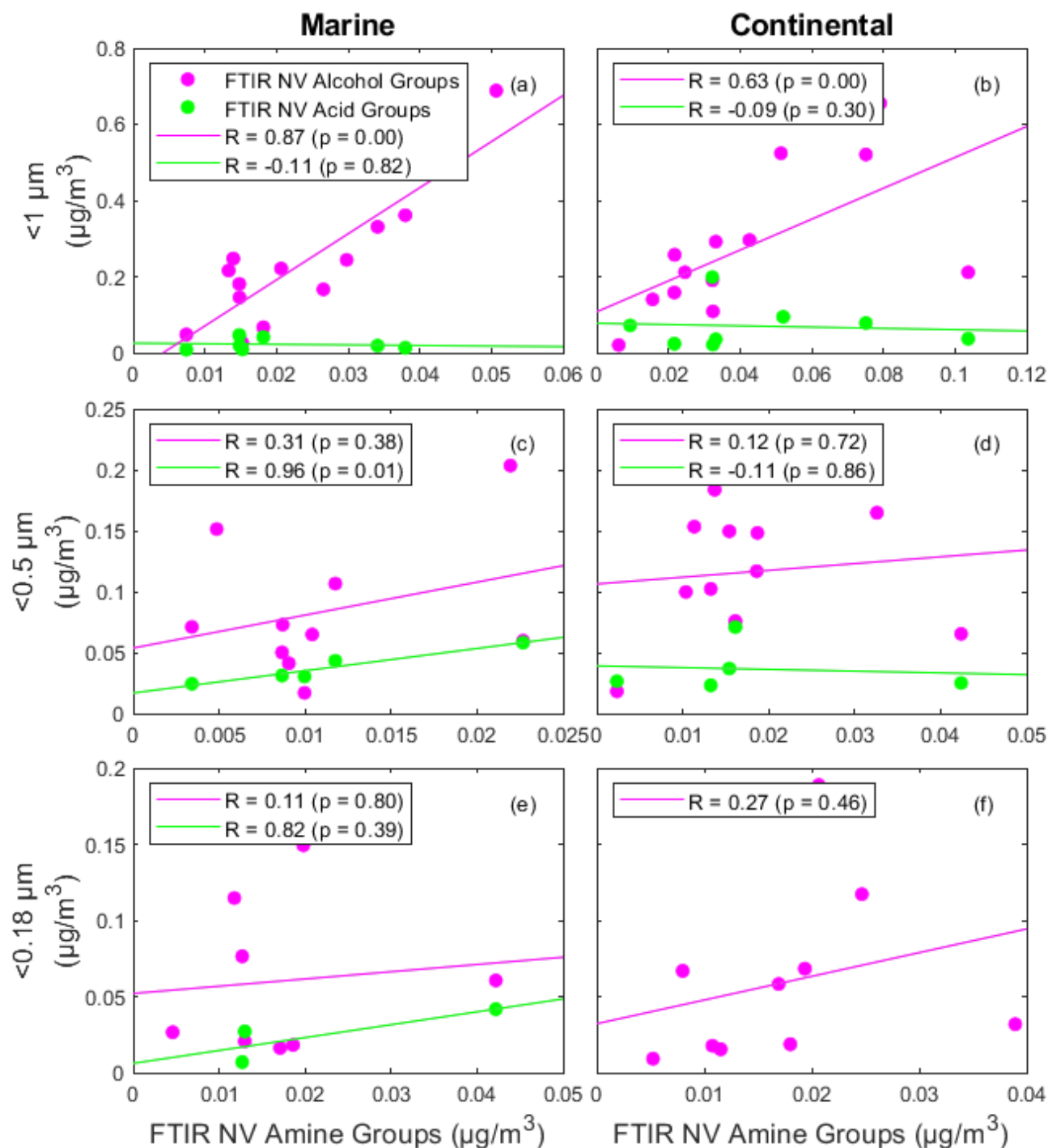
Figure 7: Scatter plot of FTIR primary (FTIR NV alcohol group: pink) and secondary (FTIR NV carboxylic acid group: green) tracers versus FTIR NV amine groups for marine filters (a,c,e) and continental filters (b,d,f) with functional group concentrations twice the standard deviation. The panels show the three filter size cut-offs: 1 μm (a,b), 0.5 μm (c,d), and 0.18 μm (e,f). The solid lines are the lines of best fit obtained using an ordinary least squares regression. A two-tailed T test is used to estimate p-values.

790
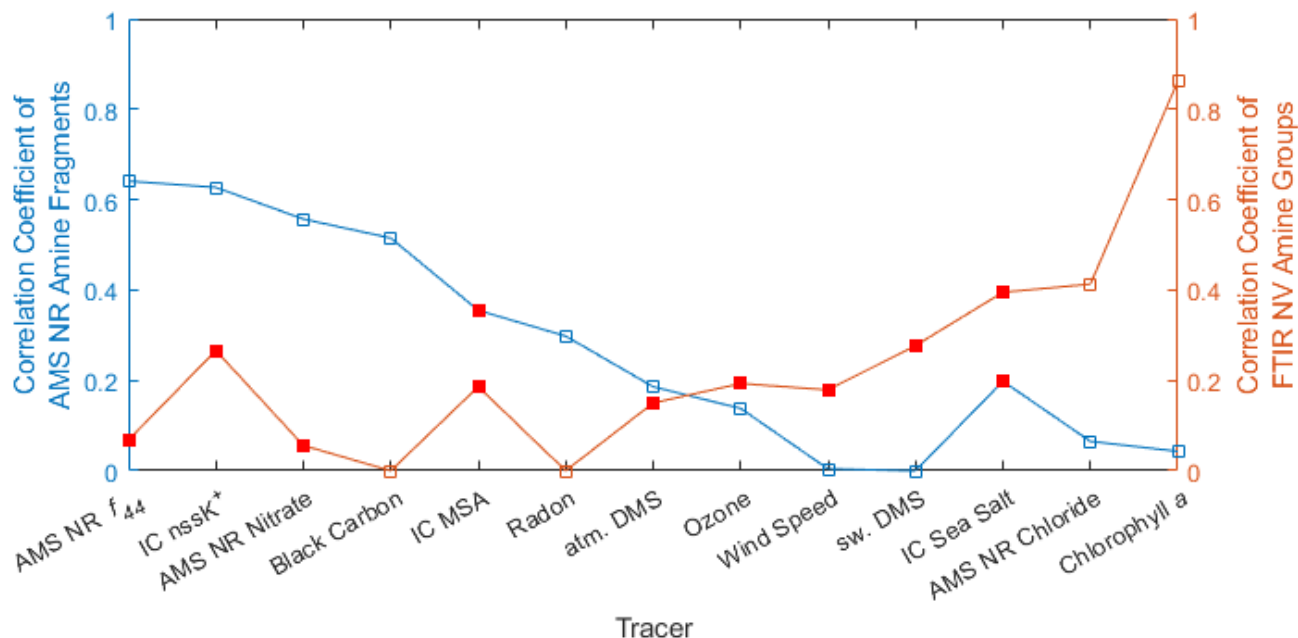
Figure 8: Plot of average Pearson correlation coefficients (R) of AMS NR amine fragments (blue) and FTIR NV amine groups in particles with diameters <1 μm (orange) with selected tracers for both marine and continental air masses. Negative correlations were averaged as 0 and only statistically significant (p < 0.05) correlations were included, except for markers shown as solid red (which were not significant). No statistically significant correlations were available for AMS NR amine fragments and IC MSA and sea salt, and for FTIR NV amine groups and all tracers with exception of black carbon, radon, AMS NR chloride, and chlorophyll *a*.

795
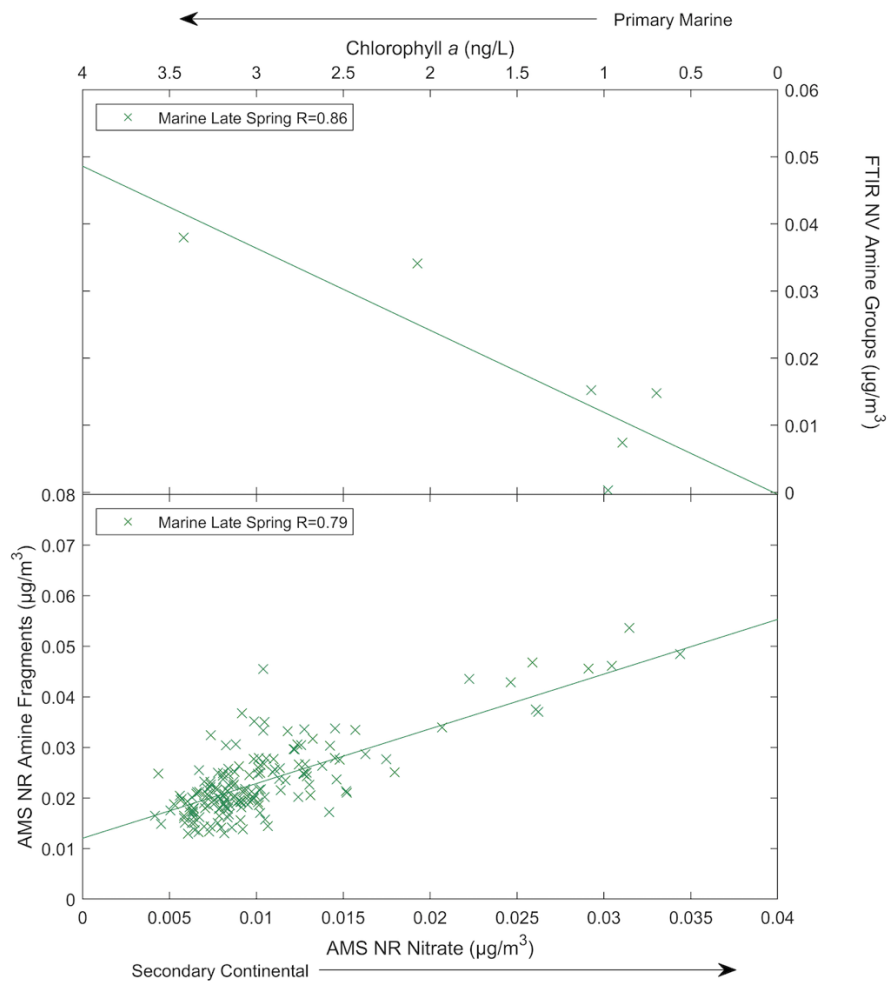
Figure 9: Scatter plot of (top) FTIR NV amine groups in particles with diameters <1 μm versus a tracer of a primary marine source (chlorophyll *a*) and (bottom) AMS NR amine fragments versus a secondary continental tracer (AMS NR nitrate) during the marine Late Spring season. The solid lines are the lines of best fit obtained using an ordinary least squares regression and a two-tailed T test is used to estimate p-values.

800